Accepted Manuscript

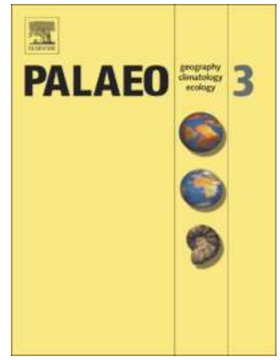

Jurassic Coastal Park: A great diversity of palaeoenvironments for the dinosaurs of the Villar del Arzobispo Formation (Teruel, eastern Spain)

Sonia Campos-Soto, Alberto Cobos, Esmeralda Caus, M. Isabel Benito, Laura Fernández-Labrador, Pablo Suarez-Gonzalez, I. Emma Quijada, Ramón Mas, Rafael Royo-Torres, Luis Alcalá

PII: S0031-0182(17)30317-6
DOI: doi: 10.1016/j.palaeo.2017.06.010
Reference: PALAEO 8326

To appear in: *Palaeogeography, Palaeoclimatology, Palaeoecology*

Received date: 21 March 2017
Revised date: 29 May 2017
Accepted date: 12 June 2017

Please cite this article as: Sonia Campos-Soto, Alberto Cobos, Esmeralda Caus, M. Isabel Benito, Laura Fernández-Labrador, Pablo Suarez-Gonzalez, I. Emma Quijada, Ramón Mas, Rafael Royo-Torres, Luis Alcalá , Jurassic Coastal Park: A great diversity of palaeoenvironments for the dinosaurs of the Villar del Arzobispo Formation (Teruel, eastern Spain), *Palaeogeography, Palaeoclimatology, Palaeoecology* (2017), doi: 10.1016/j.palaeo.2017.06.010

Jurassic Coastal Park: A great diversity of palaeoenvironments for the dinosaurs of the Villar del Arzobispo Formation (Teruel, eastern Spain)

Sonia Campos-Soto[a,b*], Alberto Cobos[c], Esmeralda Caus[d], M. Isabel Benito[a,b], Laura Fernández-Labrador[a,b,] †, Pablo Suarez-Gonzalez[e], I. Emma Quijada[f], Ramón Mas[a,b], Rafael Royo-Torres[c] and Luis Alcalá[c].

[a] Departamento de Estratigrafía, Facultad de Ciencias Geológicas, Universidad Complutense de Madrid, 28040 Madrid, Spain. sonia.campos.soto@ucm.es; mibenito@ucm.es; ramonmas@ucm.es

[b] Instituto de Geociencias IGEO (CSIC, UCM), C/ José Antonio Novais 12, 28040 Madrid, Spain

[c] Fundación Conjunto Paleontológico de Teruel-Dinópolis, Avda. Sagunto s/n, 44002 Teruel, Spain. cobos@dinopolis.com; royo@dinopolis.com; alcala@dinopolis.com

[d] Departament de Geologia (Unitat de Paleontologia), Universitat Autònoma de Barcelona, Campus Bellaterra, 08193 Cerdanyola del Vallés, Spain. esmeralda.caus@uab.es

[e] Department of Geobiology (Geoscience Centre), Georg-August-University Göttingen, Goldschmidtstraße 3, 37077 Göttingen, Germany. psuarez@uni-goettingen.de

[f] Departamento de Geología, Universidad de Oviedo, C/Jesús Arias de Velasco s/n, 33005 Oviedo, Spain. emma@geol.uniovi.es

† Deceased, April 2017

*Corresponding author. Email: sonia.campos.soto@ucm.es

Highlights

- The Villar del Arzobispo Formation includes high diversity of dinosaur fossils.

- Dinosaur ecosystems range from shallow marine to coastal and alluvial environments.

- The best preserved tracks are included in inter- to supratidal limestone beds.

- Bones are observed in siliciclastic mudstone and sandstone.

- Larger foraminifera suggest a Kimmeridgian-Tithonian age for the unit.

Abstract

The Villar del Arzobispo Formation, cropping out in the western Peñagolosa sub-basin (Late Jurassic, eastern Spain), includes abundant dinosaur tracksites and bones, which occur in diverse mixed siliciclastic and carbonate facies deposited from shallow marine to coastal and alluvial paleoenvironments. The lower part of the unit, mainly composed of bioclastic and oolitic limestone, was deposited in an inner carbonate platform, which underwent episodic subaerial exposure and siliciclastic inputs from the emergent areas, and includes scarce dinosaur tracks. This environment evolved into a siliciclastic coastal and alluvial plain that was crossed by channels and affected by periodic flooding events, producing the deposition of splay lobes. Upward, the siliciclastic coastal and alluvial deposits are interbedded with inter- to supratidal limestone beds. These tidal and coastal deposits show the highest abundance, diversity and best preservation of dinosaur tracks and bones of the unit. This setting gradually evolved upward into an inner carbonate platform, producing the deposition of shallow marine bioclastic and oolitic limestone, which includes very scarce dinosaur tracks.

The highest abundance, diversity and best preservation of theropod, sauropod, thyreophoran and ornithopod tracks occur at the top of tidal carbonate beds. Tracks also occur in the siliciclastic coastal and alluvial plain deposits, especially in the flood plain deposits, preserved, mainly, as infillings or natural casts. Additionally, very scarce and poorly-preserved tracks occur at the top of shallow marine carbonate beds. Bones may be articulated and/or associated in the flood plain deposits, whereas they are isolated and dispersed in the splay lobe deposits.

Although this unit has been previously assigned to the Tithonian-Berriasian, the analysis of larger benthic foraminifera suggests a Kimmeridgian-Tithonian age for the

Villar del Arzobispo Formation. This is consistent with the dinosaur assemblages present in the unit, which are strongly related to other European Late Jurassic faunas.

Keywords: Kimmeridgian-Tithonian, vertebrates, tracksites, foraminifera, coastal wetland, Maestrazgo Basin.

1. Introduction

The Villar del Arzobispo Formation is a mixed siliciclastic-carbonate unit that crops out throughout eastern Iberia and is internationally well-known for its abundant dinosaur fossil sites (tracks and bones), represented mainly by theropod, sauropod, thyreophoran and ornithopod fossils (Cobos *et al*., 2014 and references therein; Castanera *et al*., 2014), including those of the largest dinosaur in Europe, *Turiasaurus riodevensis* Royo-Torres, Cobos and Alcalá, 2006 and the first dinosaur described in Spain, *Aragosaurus ischiaticus* Sanz, Buscalioni, Casanovas and Santafé, 1987 (Royo-Torres *et al*., 2014). This unit has been traditionally assigned to the Late Tithonian-Middle Berriasian (e.g. Aurell *et al*., 1994; Mas *et al*., 2004) and interpreted as deposited in shallow marine to coastal and fluvial environments (e.g. Meléndez *et al*., 1979; Mas *et al*., 1984; 2004; Díaz-Molina and Yébenes, 1987; Aurell *et al*., 1994; 2016; Ipas *et al*., 2005; Luque *et al*, 2005; Santisteban and Santos-Cubedo, 2010a; 2010b; Campos-Soto *et al*., 2016a; 2016b).

This study was carried out in the western Peñagolosa sub-basin (southern Maestrazgo Basin, Teruel province, Fig. 1), where the Villar del Arzobispo Formation includes abundant dinosaur tracks and bones, although, for the moment, it is specially known for the tracks (e.g. Cobos *et al*., 2005; 2010; 2012; 2014; 2015; Alcalá *et al*., 2014a; 2014b), such as the ichnotaxa *Deltapodus ibericus* Cobos, Royo-Torres, Luque, Alcalá and Mampel, 2010 and *Iberosauripus grandis* Cobos, Lockley, Gascó, Royo-Torres and Alcalá, 2014 (stegosaurid and megalosaurid trackmakers, respectively). Dinosaur bones from this unit and sub-basin include several postcranial elements of the stegosaurid *Dacentrurus* (Cobos *et al*., 2010), sauropod remains (some of them assigned to Diplodocoidea indet, see Cobos *et al*., 2015; and others that have not been taxonomically assigned) and a large theropod tooth assigned to Megalosauridae indet

(Cobos *et al*., 2014; 2015). However, most of the in-depth study of these bones is in progress (Table 1).

Despite the importance of dinosaur fossils, no detailed mapping, or stratigraphic, sedimentological and micropaleontological studies have been performed in the area for the last 30 years, and thus, important uncertainties concerning the paleoenvironmental controls on the presence of dinosaur fossils and their accurate age are still unsolved. This multidisciplinary study analyzes in detail the diverse alluvial-coastal to shallow marine depositional paleoenvironments where dinosaurs lived and links them to the occurrence of the ichnological and osteological dinosaur fossil sites in the Villar del Arzobispo Formation. Moreover, the data presented in this work provide new findings on the dinosaur fossil-coastal record, which has been increasing over the last few years in Iberia (e.g. Lockley *et al*., 2007; 2008; Avanzini *et al*., 2012; Santos *et al*., 2013; Suarez-Gonzalez *et al*., 2013; 2015; Quijada *et al*., 2013; 2016; Castanera *et al*., 2014; Benito *et al*., 2015; Cobos *et al*., 2016; Razzolini *et al*., 2016).

Furthermore, the age of the unit has been controversial for the last decades (see Geological setting). The last detailed micropaleontological studies date back to the 70´s and 80´s (Gautier, 1968; Felgueroso and Ramírez del Pozo, 1971; Godoy *et al*., 1983; Hernández *et al*., 1985; Godoy *et al*., 1986) and, since then, no micropaleontological studies have been carried out in the studied area. In this work, we present new micropaleontological data and, for the first time in 30 years, microfossils with chrono- and biostratigraphic relevance are figured and their distribution throughout the unit is documented. The new micropaleontological data provide a new and more accurate dating for the unit and, therefore, for the dinosaur fossils that it includes.

2. Geological setting

The studied deposits belong to the Upper Jurassic-Lower Cretaceous infill of the Maestrazgo Basin (eastern Spain; Fig. 1A-B), which is one of the basins of the Mesozoic Iberian Extensional System (Salas *et al*., 2001; Mas *et al*., 2004), developed during the Late Oxfordian-Middle Albian in eastern Iberia (Salas and Guimerà, 1996; 1997; Salas *et al*., 2001; Mas *et al*., 2004). During this period, the Maestrazgo Basin had an intermediate location between the emergent areas, located to the west (Iberian Massif) and to the north (Ebro Massifs), and the open marine areas, located to the east-southeast (Tethyan realm; Fig. 1C; Salas *et al*., 2001; Mas *et al*., 2004). The Maestrazgo Basin has been divided into several sub-basins bounded by major tectonic structures (Fig. 1B; Salas and Guimerà, 1996; 1997); specifically, the studied area is located in the western Peñagolosa sub-basin (east of Teruel province), which is the southernmost sub-basin of the Maestrazgo Basin (Figs. 1B and 2; Salas and Guimerà, 1996; 1997).

The deposits studied in this work correspond to the Villar del Arzobispo Formation, a mixed siliciclastic-carbonate unit, defined by Mas *et al*. (1984), which has been interpreted as deposited in an inner carbonate platform-lagoon that evolved upward into mixed siliciclastic-carbonate coastal systems and/or into continental systems (e.g. Felgueroso and Ramírez del Pozo, 1971; Meléndez *et al*., 1979; Mas and Alonso, 1981; Mas *et al*., 1984; 2004; Díaz-Molina and Yébenes, 1987; Aurell *et al*., 1994; Luque *et al*., 2005; Ipas *et al*., 2007; Campos-Soto *et al*., 2016a; 2016b). This unit was deposited during the early stages of the Late Jurassic-Early Cretaceous extensional cycle (e.g. Salas *et al*., 2001; Mas *et al*., 2004), and thus, it was affected by syn-sedimentary faults during deposition, which controlled its significant thickness variations (e.g. Mas and Alonso, 1981; Mas *et al*., 1984; Aurell *et al*., 1994; 2016; Figs. 2 and 3).

In the studied area (western Peñagolosa sub-basin), the parastratotype of the Villar del Arzobispo was defined next to Cedrillas village (Fig. 2A; Mas *et al*., 2004) and corresponds to the sections B, C and D of the Cedrillas profile of Meléndez *et al.* (1979). These authors interpreted the Villar del Arzobispo Formation deposits as formed in a lagoon-tidal flat environment that evolved into a fluvial-lacustrine system and, subsequently, into a restricted tidal environment with beach development. Recently, Campos-Soto *et al*. (2016b) divided the unit into two informal parts: the lower part deposited in an inner carbonate platform, which episodically underwent subaerial exposure and received siliciclastic inputs from the continent, and the middle-upper part deposited in a mixed siliciclastic-carbonate coastal and alluvial plain, which evolved upward into a mixed siliciclastic-carbonate inner platform.

The Villar del Arzobispo Formation conformably overlies the Higueruelas Formation (Fig. 4A), which consists mainly of oncolitic limestone deposited in a mid- to inner-carbonate platform (e.g. Aurell 1990; Aurell *et al*., 1994; 2012; Ipas *et al*., 2004a; 2004b; 2005). The contact between both units is gradual (e.g. Mas *et al*., 1984; 2004) and, in this work, is placed at the first occurrence of sandstone beds. In the studied area, the Higueruelas Formation deposits were assigned to the Kimmeridgian (Gautier, 1968; Felgueroso and Ramirez del Pozo, 1971; Godoy *et al*., 1983) or to the Kimmeridgian-Portlandian? (Hernández *et al*., 1985) based on larger benthic foraminifera (Fig. 4B). Afterwards, the unit was assigned to the Tithonian-Early Berriasian (Aurell, 1990; Fig. 4C) or to the Tithonian in regional works (Aurell *et al*., 1994; 2002; Mas *et al*., 2004), also based on larger benthic foraminifera. The Villar del Arzobispo Formation is uncomformably overlain, toward the south of the studied area, by the Mora de Rubielos Formation (Late Berriasian-Early Valanginian in age according to Salas *et al*., 2001; Mas *et al*., 2004; Figs. 2 and 4A), which is a coarse siliciclastic unit deposited in a coastal alluvial system (e.g. Moissenet and Gautier, 1971; Canerot *et al*., 1982; Godoy *et al*., 1986). Toward the north of the studied area, the Villar del Arzobispo Formation is overlain by the El Castellar Formation (Late Hauterivian-basal Barremian in age according to Gautier, 1981; Martín-Closas, 1989; Late Valanginian-Hauterivian in age according to Salas *et al*., 2001; Mas *et al*., 2004; Figs. 2 and 4A), which consists of a mixed carbonate-siliciclastic unit deposited in a fluvial-lacustrine environment with marine influence (e.g. Canerot *et al.*, 1982; Salas, 1987).

The age previously assigned to the Villar del Arzobispo Formation in the studied area is controversial. Gautier (1968), Felgueroso and Ramírez del Pozo (1971), Hernández *et al*., (1985) and Godoy *et al*., (1986) attributed a Late Kimmeridgian-Portlandian age to the unit (Fig. 4B) based on the larger benthic foraminifera assemblage dominated by *Kurnubia palastiniensis* Henson, *Everticyclammina virguliana* (Koechlin), *Rectocyclammina arrabidensis* Ramalho, *Pseudocyclammina gr. parvula-maluchensis* Hottinger, *Nautiloculina oolithica* Mohler, *Pseudocyclammina gr. lituus* (Yokoyama), *Labyrinthina mirabilis* Weynschenk and *Trocholina alpina* Leupold at its base and *Anchispirocyclina lusitanica* (Egger) in its uppermost part. However, Godoy *et al.* (1983) attributed the unit to the Late Kimmeridgian?-Early Valanginian (stages referred to the Boreal regional stages; Fig. 4B). Aurell (1990) indicated a "Portlandian (i.e. Early and Middle Berriasian)" age, although afterwards, in some regional works, Aurell *et al*. (1994) and Mas *et al*. (2004) attributed the unit to the Late Tithonian-Middle Berriasian (Fig. 4C), also based on the same foraminiferal assemblage mentioned above. Campos-Soto *et al*. (2016a) re-studied the foraminiferal assemblage from the lower part of the unit in the northwestern South Iberian Basin, suggesting a Kimmeridgian age due to the presence of *Alveosepta personata.*

Afterwards, Campos-Soto *et al*. (2016b) analyzed the foraminiferal assemblage of the carbonates of the upper part of the unit in the western Peñagolosa sub-basin and assigned it provisionally to the interval Late Tithonian-earliest Berriasian? due to the presence of *Anchispirocyclina lusitanica*. In parallel, Aurell *et al*. (2016) attributed the deposits of the Villar del Arzobispo Formation in the Peñagolosa sub-basin (*sensu* Cobos *et al*., 2010; 2014) to the Middle Tithonian-Middle Berriasian (Fig. 4C), and consider the deposits of the upper part of the succession, as equivalent to a new lithostratigraphic unit, which they define in the adjacent Galve sub-basin (Fig. 1B).

3. Methodology

This work was based on detailed geological mapping, as well as stratigraphic, sedimentological and paleontological analysis of the Villar del Arzobispo Formation in the studied area. Geological mapping of the studied area was carried out using field observations, satellite images and aerial photographs (Fig. 2A-B). During geological mapping, special emphasis was laid on the limestone beds, meticulously mapping them throughout the studied area (Fig. 2A-B). ArcGIS software was used to integrate and georeference the cartographic data.

Four detailed stratigraphic sections of the Villar del Arzobispo Formation were logged in the areas with best outcrop conditions (Figs. 2A and 3): Cedrillas section (CE), El Castellar section (CAS), Formiche Alto section (FA) and Mora de Rubielos section (MO) with 735 m, 555 m, 1383 m and 108 m of thickness, respectively. The Villar del Arzobispo Formation crops out completely in the CE, CAS and FA sections, whereas in the MO section only its uppermost part is represented due to a fault (Figs. 2A and 3). Numerous additional outcrops of the unit were studied in order to complete the geological mapping, to analyze the lithology, fossil content, geometry and lateral continuity of the deposits, to acquire paleocurrent data and to study the dinosaur fossils and their relationship with the deposits in which they are included. Paleocurrent data values (Fig. 3) were obtained subtracting the tectonic dip.

A total of 305 rock samples were collected systematically along the stratigraphic sections and in other outcrops of the studied area. From each collected sample, a polished and uncovered thin section (30 μm thick) was prepared for petrological study under transmitted-light microscopy. The classification of carbonate rocks of Dunham (1962) and the classification of siliciclastic rocks of Zuffa (1980) were used for petrographic and sedimentological descriptions.

The micropaleontological and biostratigraphical studies are based on larger benthic foraminifera (LBF) from 33 samples of carbonate rocks from several stratigraphic levels of the CE, CAS and MO sections (CE, CAS and MO samples, respectively) and only one level of the FA section (SP sample; Fig. 3). Some samples from the underlying Higueruelas Formation (CE and CAS sections) have also been studied for comparing the evolution and replacements of the LBF assemblages in successive stratigraphic levels. From the collected samples, 39 thin-sections have been prepared in order to obtain information on the LBF architectural and structural features in random sections. If possible, LBF are identified at genus and species level; in LBF the genera are defined by the presence or absence of structural elements combined with the chamber arrangement, while the species are defined by quantitative parameters. The biostratigraphic ranges reported for the identified taxa in the specialized literature are also discussed.

This work includes all the main dinosaur sites inventoried in the studied area (Table 1) by the Fundación Conjunto Paleontológico de Teruel-Dinópolis since 2002. They have been georeferenced according to the reference system ETRS89/ UTM Zone

30N (Fig. 2A-B) and their exact coordinates are recorded in the Dirección General de Cultura y Patrimonio del Gobierno de Aragón.

4. Depositional paleoenvironments of the dinosaur fossil-bearing deposits

The Villar del Arzobispo Formation at the studied area has been divided into two main parts (*sensu* Campos-Soto *et al*., 2016b), which record different abundances of dinosaur tracks and bones (Fig. 3, Table 1).

1) The lower part comprises alternating bioclastic, oolitic and peloidal limestone, containing abundant marine fossils, siliciclastic mudstone, sandstone and very scarce conglomerate (Figs. 3 and 5A-B). The thickness of the lower part increases southwards (Fig. 3). Dinosaur fossils in the lower part are very scarce (Fig. 3, Table 1).

2) The middle-upper part includes the greatest abundance and diversity of dinosaur fossils of the unit (Fig. 3, Table 1). It is formed by siliciclastic mudstone interbedded with sandstone, limestone and minor conglomerate (Figs. 3 and 5C-E). Generally, limestone beds are progressively more abundant and include more marine fossils toward the upper part of the unit (Fig. 3). However, some differences have been observed between the northern and southern sectors of the studied area. In the northern sector (CE and CAS sections), limestone beds are only observed toward the upper part of the unit (Figs. 3 and 5C); whereas, in the southern sector (FA section), where the thickness of the middle-upper part significantly increases compared to the northern sections (Fig. 3), limestone beds are interbedded with siliciclastic deposits throughout the middle-upper part of the unit (Fig. 3). Moreover, in the southern sector (FA and MO sections) there is an increase of fossils indicative of normal marine salinity, such as corals, echinoderms, red and dasyclad algae, compared to the northern sector (Fig. 3).

Additionally, the lower and middle-upper parts of the unit include different assemblages of microfossils, which allow to shed light on the age of the unit and, thus, of the dinosaur fossils that it includes, and will be analyzed in section 6.

Dinosaur fossils (tracks and bones) occur in most carbonate and siliciclastic deposits of the Villar del Arzobispo Formation (Fig. 3). The stratigraphical position and paleoenvironmental interpretations of the deposits that include the different types of dinosaur fossils are explained below and summarized in Table 1:

4.1. Carbonate deposits

Carbonate deposits consist on bioclastic, oolitic and peloidal limestone (Fig. 6A-F) and mudstone and peloidal limestone (Fig. 6G-M). Both are interbedded with siliciclastic mudstone and non-channelized sandstone bodies (Fig. 3).

4.1.1. Bioclastic, oolitic and peloidal limestone

Bioclastic, oolitic and peloidal limestone is observed in the lower and upper parts of the unit in the northern sections (CE and CAS), throughout the FA section (although they are still most abundant in the lower and upper parts), and in the MO section, which only records the uppermost part of the unit (Figs. 2, 3 and 6A-F). It is interbedded with siliciclastic mudstone, non-channelized sandstone bodies and locally with marl (Fig. 3).

Bioclastic, oolitic and peloidal limestone is arranged in decimeter to meter thick beds (0.20-7.80 m, Figs. 5A-B, E and 6A-B) and displays great lateral continuity (from 80 m to more than 11 km, Fig. 2A). Microscopically, limestone commonly shows a well-sorted packstone-grainstone texture (Fig. 6C) made up of ooids, bioclasts (small and large agglutinated forams, small miliolids, fragments of ostreids and other bivalves, echinoderms, ostracods, serpulids, gastropods, dasyclad and red algae, scarce decimeter-scale fragments of corals, inoceramids, and charophytes), homogeneous fecal pellets, carbonate intraclasts, quartz grains and scarce oncoids and plant remains. Quartz grains may be locally abundant. Some limestone beds may show abundant poorly-sorted, large bioclast fragments (ostreids, inoceramids and other bivalves, gastropods and serpulids up to 8 cm in size; Fig. 6D-E). Limestone beds commonly display abundant burrowing, among which *Rhizocorallium*- (Fig. 6F) and *Thalassinoides*-like traces have been distinguished; moreover, toward the lower part of the unit in the northern CE and CAS sections, they may show edaphic features, such as irregular, brecciated and ferruginous tops (Fig. 3). Additionally, dinosaur tracks have locally been observed at the top of some beds (see section 4.1.3).

Sedimentary features of the bioclastic, oolitic and peloidal deposits (the packstone-grainstone texture and the fossil content) suggest that deposition took place in a shallow to very shallow carbonate inner platform, above the fair-weather wave-base and under normal marine salinity waters. This platform was affected by the action of storms as suggested by the presence of some limestone beds containing large and poorly-sorted bioclast fragments. Freshwater and siliciclastic inputs from the emergent areas arrived at the carbonate platform, as indicated by the occurrence of sandstone, siliciclastic mudstone and marl interbeds, as well as by the presence of sparse fragments of charophytes and occasionally abundant quartz grains. In addition, the inner carbonate platform underwent episodic subaerial exposure, to the northern sector of the studied area, as shown by the presence of edaphic features (i.e. irregular, brecciated and ferruginous tops). This interpretation is consistent with that given by Campos-Soto *et al*. (2016a) for similar marine limestone deposits of the Villar del Arzobispo Formation in the northwestern South Iberian Basin (Fig. 1A).

4.1.2. Mudstone and peloidal limestone

Mudstone and peloidal limestone, which is interbedded with siliciclastic mudstone (Figs. 3 and 5C-D), is observed in the upper part of the northern sections (CE and CAS sections), in the middle part of the FA section and in the uppermost part of the MO section (Figs. 2, 3 and 6G-M).

Mudstone and peloidal limestone is arranged in decimeter to meter thick beds (0.40-4 m thick; Fig. 6G-H), which may display great lateral continuity (from 75 m to at least up to 6 km; Fig. 2A-B). Internally, limestone beds are commonly laminated and are composed of alternating millimeter- to centimeter-thick layers of mudstone and peloidal packstone-grainstone textures, displaying flaser, wavy and lenticular bedding (Fig. 6I). In addition, other limestone beds may be entirely formed by mudstone or packstone-grainstone deposits. Mudstone is formed by dense micrite, scarce quartz grains and very scarce fragments of ostracods, echinoderms, small agglutinated forams, small miliolids, fecal pellets, intraclasts and ooids (Fig. 6J). Bioturbation (horizontal and vertical burrows of 0.8 mm to 3.75 mm in size, commonly filled by fecal pellets), fenestral porosity (Fig. 6J) and nodules with circumgranular cracks are commonly observed in the mudstone deposits. Peloidal packstone-grainstone is commonly well sorted and is composed of fine homogeneous fecal pellets (60-280 μm), quartz grains, minor micritic intraclasts and scarce fragments of ostracods, echinoderms, small agglutinated forams, small miliolids, ostreids and other bivalves, ooids, and plant remains (Fig. 6K). Current and wave ripples, as well as burrows (horizontal and vertical traces of 1.5 mm to 4 mm in size and filled by fecal pellets), and occasional fenestral porosity are observed in the peloidal deposits. Millimeter- to centimeter-thick layers of silt to fine-grained sandstone, displaying current ripples, are locally interbedded with the mudstone and peloidal limestone.

Rhizocorallium and *Diplocraterion*-like traces, as well as millimeter-sized burrows (Fig. 6L), which commonly display vertical traces and locally horizontal traces, have been observed at the top of some bed surfaces. Moreover, the top of some beds displays patched dark-grey and light-grey colors, including abundant millimeter-sized burrows (Fig. 6L). In detail, light-grey patches are composed of millimeter to sub-millimeter thick mudstone layers, which overlie the dark-grey layers. Burrowed light-grey patches are similar to those reported by Alcalá *et al*. (2014b) for the same limestone beds of the Villar del Arzobispo Formation and to those documented by Cariou *et al*. (2014) in the Upper Jurassic record of the French Jura Mountains, being in both cases interpreted as microbial mats. Desiccation cracks (Fig. 6M), which may be observed at the top of several and consecutive centimeter- to decimeter-thick layers, edaphic features (irregular and brecciated tops and root traces) and abundant dinosaur tracks (see section 4.1.3.) are also common at the tops of beds.

Features of the mudstone and peloidal limestone deposits, such as their fossil content, the occurrence of bioturbation (*Rhizocorallium* and *Diplocraterion*-like traces), fenestral porosity, abundant desiccation cracks and edaphic features, suggest that deposition took place in shallow to very shallow water bodies of normal marine to brackish salinities. These features, together with the great lateral continuity of these deposits and with the occurrence of flaser, wavy and lenticular bedding suggest deposition in the inter- to supratidal zone (e.g. Shinn, 1983a; 1983b; Demicco and Hardie, 1994; Nagy *et al*. 2005) of a broad and low gradient carbonate tidal flat, which underwent periodic desiccation and flooding (e.g. Tebbutt *et al*., 1965; Hanley and Steidtmann, 1973; Grover and Read, 1978; Shinn, 1983a), and which was colonized by typical marine burrowers (as indicated by the occurrence of *Rhizocorallium*- and *Diplocraterion*- like traces; e.g. MacEachern *et al*., 2007). Siliciclastic inputs from the continent arrived to these coastal areas, as suggested by the presence of thin layers of rippled sandstone interbedded with limestone beds. A tidal flat environment has also been interpreted by Alcalá *et al*. (2014b) for the limestone beds that include dinosaur tracksites of El Castellar (CT-1), El Pozo (CT-2) and Camino El Berzal (CT-3; Figs. 2 and 3), based on the occurrence of alternating massive micritic layers with peloidal layers, algal mats (displaying birds-eye vugs, tepees, chip mats and desiccation shrinkage marks) and silty layers, locally displaying herring-bone cross-bedding, and also based on the presence of ostreids, gastropods and fish scales.

4.1.3. Dinosaur fossils in carbonate beds

Dinosaur tracks are common in the mudstone and peloidal limestone beds, whereas they are very scarce in the bioclastic, oolitic and peloidal limestone beds (Figs. 3 and 7). Osteological remains have not been found in these deposits.

Mudstone and peloidal limestone beds include abundant dinosaur tracks, which have been the subject of several systematic paleontological studies in the considered area (Cobos *et al*., 2005; 2008; 2010; 2012; 2015; Alcalá *et al*., 2014a; 2014b). The majority of the tracks occur at the tops of mudstone and peloidal limestone beds (Fig. 7A-H), whereas very scarce recognizable tracks are present at the bases of beds (Fig. 7I). Dinosaur tracks observed at the tops of mudstone and peloidal limestone beds are typically associated with desiccation cracks (Fig. 7A, C) and occasionally with wave ripples. Tracks also occur at the top of limestone beds displaying deformed and burrowed light-grey patches, which are interpreted as microbial mats (Alcalá *et al*., 2014b; Fig. 7F). In addition, root traces have been locally observed at the top of some limestone beds containing tracks. These features indicate that sauropod, thyreophoran, ornithopod and theropod dinosaurs walked on the inter- to supratidal areas of the coastal plain, which underwent periodic flooding and subaerial exposure.

Dinosaur tracks observed at the top of mudstone and peloidal limestone beds show different degrees of preservation: 1) Very well-preserved tracks: display well-defined shapes, are generally shallow, have vertical walls, do not generally show displacement rims (Fig. 7A-B) and may show anatomical details, such as foot pads impressions and/or claw marks (Fig. 7B). Similar features have been described in tracks of both modern (Allen, 1997; Marty, 2008; Marty *et al*., 2009) and ancient tidal flats (Marty, 2008), and have been interpreted as produced in substrates with stiff consistency and moderate moisture content and strength. 2) Well-preserved tracks: show moderately to well-defined shapes, are generally deep, show large, wide, prominent, rounded and well-defined displacement rims and may display vertical walls (Fig. 7C-E). According to Allen (1997), Marty (2008) and Marty *et al*. (2009), tracks displaying these features are commonly produced in soft substrates with high moisture content and low strength. 3) Poorly-preserved tracks: show moderately to poorly defined shapes, are commonly shallow and display contoured, wide and poorly-defined displacement rims (Fig. 7F). Theses tracks were described by Alcalá *et al*. (2014b) in the dinosaur site of El Pozo (CT-2), and have been interpreted as produced in a low cohesion substrate with great water content. 4) Very poorly-preserved tracks: show poorly defined outlines, are shallow to very shallow and commonly do not display displacement rims (Fig. 7G-H). This type of tracks is similar to those described in modern (Allen, 1997; Marty, 2008; Marty *et al*., 2009) and ancient tidal flats (Marty, 2008; Alcalá *et al*., 2014b; Cariou *et al*., 2014), and have been interpreted as produced in substrates with low water content and high strength.

Additionally, poorly-preserved dinosaur tracks are also observed at the base of scarce mudstone and peloidal limestone beds, which are preserved as convex hyporeliefs (natural track casts; Fig. 7I). They display elongated shapes and show a massive sediment infill, which is mainly made up of peloids, quartz grains and scarce marine fossils and ooids. Tracks may penetrate up to 20 cm in the underlying reddish siliciclastic mudstone, which displays edaphic features (such as root traces and carbonate nodules). These features indicate that the production of tracks occurred on the siliciclastic muddy sediment, which was subaerial exposed. The muddy substrate should have had the sufficient moisture content to make the production of tracks of several cms deep possible, because if the mud was dried at the moment of the production, the tracks would have consisted of very shallow and flat traces (Allen, 1997; Marty, 2008; Marty *et al*., 2009).

Bioclastic, oolitic and peloidal limestone (Fig. 7J-K) locally includes sparse and poorly-preserved dinosaur tracks. They are locally observed at the tops of some beds in the lower and upper parts of the unit (sites CT-68 and CD-2; Figs. 2, 3 and 7J) and as a natural cast in the uppermost part of the unit, filled by massive bioclastic, oolitic and peloidal limestone (site MR-10; Figs. 2, 3 and 7K). The occurrence of these tracks indicates that dinosaurs also stepped on very shallow inner carbonate platform deposits. The poor preservation suggests that the water content of the original sediment was high (e.g. Allen, 1997; Alcalá *et al*., 2014b), which is consistent with the fact that features indicative of subaerial exposure (i.e. desiccation cracks, irregular and/or brecciated tops) have not been observed in the deposits including these tracks.

4.2. Siliciclastic deposits

Siliciclastic deposits are observed all along the Villar del Arzobispo Formation (Figs. 3 and 5), although they are more abundant in the middle-upper part of the unit. They comprise siliciclastic mudstone (Fig. 8A-C), non-channelized sandstone bodies (Fig. 8D-H), and minor channelized sandstone and conglomerate bodies (Fig. 8I-K).

4.2.1. Siliciclastic mudstone

Siliciclastic mudstone is the most abundant facies of the Villar del Arzobispo Formation (Fig. 8A-C). It is present throughout the unit, although it is most abundant and thickest in the middle-upper part (Fig. 3). It is interbedded with non-channelized sandstone bodies, channelized sandstone and conglomerate bodies, and with carbonate beds (both bioclastic, oolitic and peloidal limestone and micritic and peloidal limestone; Fig. 3).

Siliciclastic mudstone is typically reddish-colored and commonly displays edaphic features, such as green mottling, carbonate nodules and root traces (Fig. 8A-C). Most of the dinosaur bones have been observed in the siliciclastic mudstone (see section 4.2.4.).

Siliciclastic mudstone features indicate deposition on a broad flood plain (e.g. Collinson, 1996; Miall, 1996), which underwent periods of subaerial exposure and paleosol development (e.g. Freytet and Plaziat, 1982; Alonso-Zarza and Wright, 2010). The flood plain was located in coastal areas as suggested by the alternation of siliciclastic mudstone deposits with shallow marine and inter- to supratidal carbonates. This is similarly observed in modern coastal settings, such as in the Malaysian Klang River Delta, where coastal flood plain areas are laterally related with tidal flats and swamps (Coleman, 1976). This relationship is also observed in the Burdekin Delta

(Australia), which consists of a mosaic of different sub-environments, including flood plains, swamps, tidal flats, beaches and shallow marine areas (Coleman, 1976).

4.2.2. Non-channelized sandstone bodies

Non-channelized sandstone bodies are observed throughout the Villar del Arzobispo Formation interbedded with siliciclastic mudstone and limestone (Fig. 3). In the lower and upper parts of the unit, where they are also interbedded with bioclastic, oolitic and peloidal limestone (Figs. 3 and 5A-B, E), they may locally contain up to 15% of marine bioclasts (small and large agglutinated forams, fragments of ostracods, echinoderms, ostreids and other bivalves), carbonate intraclasts and ooids.

Non-channelized sandstone bodies are arranged in decimeter to meter thick beds (Fig. 8D-H). The thickest non-channelized sandstone bodies (3-9 m thick) commonly show a coarsening- and thickening-upward trend, display flat bases and tops (Fig. 8D-E) and commonly display great lateral extent (up to 210 m). Toward the base, they comprise centimeter to decimeter thick layers of very fine- to fine-grained sandstone (displaying current ripples) alternating with siliciclastic mudstone, which change upward to meter thick layers of fine- to medium-grained sandstone displaying parallel lamination, large-scale cross-bedding and sigmoidal cross-bedding (paleocurrent data indicate a transport toward the NE; Fig. 3).

Additionally, there are other non-channelized sandstone bodies, which commonly exhibit thinner thicknesses (0.1-4.30 m thick; Fig. 8F-H), do not show any grain size variation or any thickening-upward trend, but still show flat bases, convex or flat tops (Fig. 8H) and commonly display limited lateral continuity (commonly 10-60 m and locally up to 100 m; Fig. 8H). These beds are predominantly fine- to medium-grained along the unit, although some coarse-grained beds have also been observed in the middle-upper part of the unit. These beds display parallel lamination, large-scale cross-bedding (sets up to 1.30 m thick), sigmoidal cross-bedding and minor current ripples. Paleocurrent data indicate a main transport toward the NE-SE and occasionally toward the NW-SW (Fig. 3). These non-channelized sandstone bodies may contain millimetric and centimetric plant remains (including fragments of fossil trunks up to 25 cm in size); may display yellow, orange, red and green mottling and, toward the top of the beds, they may show root traces and bioturbation.

Non-channelized sandstone bodies may include dinosaur tracks and bone remains (see section 4.2.4). Tracks are commonly observed at the base of beds, although they locally occur at the top of beds, whereas bones are dispersed within non-channelized sandstone bodies.

Non-channelized sandstone bodies, interbedded with siliciclastic mudstone and shallow marine and tidal limestone, are interpreted as overbank deposits formed as splay lobes (*sensu* Collinson, 1996; Miall, 1996) in a coastal and alluvial plain, as suggested by the geometry (flat bases and flat to convex tops) and the coarsening and thickening upward trend (*cf*. Coleman, 1976; Farrel, 1987; Miall, 1996; McKie, 2011). Similar deposits have previously been reported as produced during flood events in other ancient and modern coastal (e.g. Coleman, 1976; Coleman and Prior, 1982; Farrell, 1987; Ataol, 2015) and alluvial settings (Turner, 1986; Collinson, 1996; Miall, 1996; McKie, 2011), and have been interpreted as deposited by the deceleration and expansion of a non-confined flow that comes from the overbanking of a channel (Miall, 1996). The thinner non-channelized sandstone bodies displaying limited lateral extent, flat bases and convex or flat tops, would have been deposited during episodic floods, according to Turner (1986) and Farrell (1987); the thicker non-channelized sandstone bodies displaying coarsening- and thickening-upward trends and great lateral extent would have been deposited as the result of the progradation of splays during "long term" floods, according to Coleman (1976), Coleman and Prior (1982), Turner (1986) and McKie (2011). Moreover, the sigmoidal cross-bedding observed in some sandstone beds suggests progradation of the splay lobes into standing and ephemeral water bodies (*cf.* Mutti *et al*., 1996; Turner and Tester, 2006; Ethridge, 2011).

Similarly, non-channelized sandstone bodies interbedded with bioclastic, oolitic and peloidal limestone beds and locally containing up to 15% of marine bioclasts are interpreted as splay lobes deposited in a shallow marine environment. In this sense, several examples of splay lobes entering in shallow marine areas have been reported in actual deltaic settings, such as in the Ceyhan Delta (Ataol, 2015) and in the Mississippi Delta (Coleman, 1976; Coleman and Prior, 1982).

4.2.3. Channelized sandstone and conglomerate bodies

Channelized sandstone and conglomerate bodies are observed in the lower and middle-upper parts of the unit, although they are more abundant in the middle part (Fig. 3), and are interbedded with siliciclastic mudstone. Dinosaur fossils have not been found in these deposits until present.

Channelized sandstone and conglomerate (Fig. 8I-K) occur as fining upward bodies of 0.30 m to 9.20 m in thickness and up to 40 m of lateral continuity, which display concave and erosive bases and flat tops (Fig. 8I-J). The lower part consists of poorly-sorted clast- or matrix-supported conglomerate made up of angular to sub-rounded carbonate and muddy soft pebbles (Fig. 8K) and minor rounded to sub-rounded quartzite pebbles (0.5-6 cm) within a medium to coarse-grained sandy matrix. Fragments of fossil trunks (up to 10 cm in size) may be common. Conglomerate changes gradually upward to coarse- to medium-grained sandstone. Sandstone may be massive or display large-scale cross-bedding (sets up to 70 cm thick), and may contain millimeter-sized plant remains. Paleocurrent data indicate a main transport toward the NE-SE and occasionally toward the S-SW (Fig. 3). Locally, conglomerate layers with limited lateral extent and up to 50 cm thick are also observed between cross-bedded sandstone.

Channelized conglomerate and sandstone bodies are interpreted as the result of channel migration across the coastal and alluvial plain as suggested by the erosive basal surfaces, the large-scale cross-bedding, the fining upward trend observed in the deposits and their alternation with siliciclastic mudstone flood plain deposits (*cf*. Reineck and Singh, 1973; Collinson, 1996; Miall, 1996; McKie, 2011). Muddy and carbonate pebbles are interpreted as intraformational clasts that probably came from the erosion and reworking of deposits formed in adjacent environments (e.g. Turner, 1986; Deluca and Erikson, 1989; Collinson, 1996; Cain and Mountney, 2009; Plink-Bjorklund, 2015). Moreover, conglomerate layers that are locally interbedded with sandstone layers suggest fluctuations of flow conditions and may have been deposited during high-energy flow episodes (e.g. Deluca and Erikson, 1989).

4.2.4. Dinosaur fossils in siliciclastic beds

Siliciclastic deposits include dinosaur bones and tracks. Bones commonly occur both in siliciclastic mudstone (Fig. 9A-C) and in non-channelized sandstone bodies (Fig. 9D-G). In the case of the siliciclastic mudstone, deposited in a flood plain, osteological remains are commonly associated and/or articulated, such as in San Cristóbal (CT-28) and La Tejería sites (CT-30; Fig. 9A), which include fossils of stegosaurs (Cobos *et al*., 2010) and sauropods, respectively. Moreover, the largest theropod tooth described in Spain (Cobos *et al*., 2014; 2015) was found *ex situ* and may have come from a nearby outcrop of siliciclastic mudstone deposits (FA-5 site, Table 1). The non-channelized sandstone bodies, interpreted as splay lobe deposits formed during flooding events, include isolated and dispersed bone remains (Fig. 9D-G).

Dinosaur tracks are also present in the non-channelized sandstone bodies (Fig. 10A-I). They are more abundant and better preserved at the base of sandstone beds overlying siliciclastic mudstone deposits (Fig. 10A-D), whereas they are scarcer and more poorly-preserved at the top of sandstone beds (Fig. 10G-I). In this sense, mud has been reported in previous works as the substrate that best preserves footprints due to its cohesiveness (e.g. Currie *et al*., 1991; Allen, 1997), whereas the potential of footprint preservation in sandy deposits is worse due to their looseness and unconsolidated character in both wet and dry conditions (e.g. Laporte and Behrensmeyer, 1980; Allen, 1997). Similarly, Lockley and Hunt (1994) and Lockley (2003) documented that the same type of tracks showed different morphology and preservation when they were made as deep casts in yielding mud filled by sand and when they were made as shallower tracks in the top of less-compactable sand beds.

Dinosaur tracks occurring at the base of non-channelized sandstone bodies are preserved as convex hyporeliefs (natural track casts), which show elongated or rounded shapes (Fig. 10A-B, D). They may penetrate up to 21 cm into the underlying sediment, which commonly consists of siliciclastic mudstone (Fig. 10D) and occasionally of alternating siliciclastic mudstone and centimeter to decimeter thick layers of very fine- to fine-grained sandstone (Fig. 10A-B). The infilling is commonly massive or may be slightly laminated (Fig. 10B). Natural track casts may show impressions of slide marks (parallel striations) made by skin scales (Fig. 10B-C), recording the movement of the feet during track-making (e.g. Gatesy, 2001; Difley and Ekdale, 2002; Avanzini *et al*., 2012; Cobos *et al*., 2016). These natural track casts are infillings of true tracks showing slide marks or grooves, which reveal the trajectory of the tracksmaker´s foot within the sediment, and which were defined as "*4D tracks"* by Cobos *et al*. (2016). Skin ornamentation has not been observed in the studied natural track casts. Moreover, some natural track casts may also record the clear outline of digit traces (Fig. 10E). Properties of the muddy substrate when the footprints were produced, such as the moisture content and strength, controlled the potential of preservation of anatomical details (such as striations or digit traces), according to Allen (1997). This author suggested that substrates characterized by moderate to low moisture content and moderate to high strength favors a fine preservation of anatomical details, such as striations and impressions of claws and skin. After footprint production, the muddy substrate desiccated and became hard enough (*sensu* Allen, 1997) that footprints were not eroded by the subsequent flooding event, but rather they were filled by them, and thus, preserved.

Dinosaur tracks locally observed at the top of non-channelized sandstone bodies are preserved as concave epireliefs (Fig. 10G-I). Tracks may penetrate up to 15 cm in the underlying sandstone layers, which are deformed in the contact with the infillings (Fig. 10G-H). The infilling is composed of siliciclastic mudstone (Fig. 10H) or occasionally of sandstone (Fig. 10G). Beds including the tracks may display edaphic features (root traces and yellow, orange, red and green mottling) and/or bioturbation and, additionally, they may be overlain by a thin layer of siliciclastic mudstone (Fig. 10H). This type of tracks is interpreted as produced after flooding and deposition of sandy splay lobes and occurred after the sandy deposits were subaerially exposed.

5. Paleoenvironmental evolution of the Villar del Arzobispo Formation and its relationship with the abundance and preservation of dinosaur fossils

Dinosaur fossils occur throughout the Villar del Arzobispo Formation, but they are more abundant and better preserved in the middle-upper part of the unit (Fig. 3). Their abundance and preservation is strongly related to the depositional paleoenvironments recorded in the unit (Fig. 11), as well as to their vertical and lateral evolution, controlled by the interplay between tectonics and eustatism.

The lower part of the unit was deposited in an inner-carbonate platform, which underwent only episodic subaerial exposure and siliciclastic inputs from the emergent areas. In this context, dinosaur tracks are very scarce and poorly preserved (Fig. 3, 7J), because this shallow marine environment would have remained subaqueous most of the time, preventing the formation and preservation of tracks. Tracks were only formed and preserved in areas of the platform that were episodically subaerially exposed, although the high water content of the sediment in these areas controlled their poor preservation.

The middle part of the unit records the upward evolution of these shallow marine environments into a coastal and alluvial plain, as suggested by the progradation of siliciclastic deposits over the carbonate-siliciclastic deposits of the lower part of the unit (Fig. 3). According to paleocurrent data (with most common directions toward the NE-SE; Fig. 3), siliciclastic deposits probably came from the Iberian and Ebro Massifs, which were respectively located to the west and north of the Peñagolosa sub-basin (Fig. 1C; e.g. Salas *et al*., 2001; Mas *et al*., 2004). The coastal and alluvial plain was subaerially exposed and crossed by channels (Fig. 11). This environment was affected by periodical flood events, leading to the deposition of splay lobes (Fig. 11). Upward, inter- to supratidal mudstone and peloidal carbonate deposits were progressively interbedded with the coastal and alluvial plain siliciclastic sediments (Figs. 3 and 11). This coastal setting, equivalent to a coastal wetland system *sensu* Suarez-Gonzalez *et al.* (2015), was very suitable for the development of dinosaur faunas and for the preservation of their fossils (including both tracks and bones; Fig. 11), as the middle part of the unit records more dinosaur tracks in both siliciclastic and carbonate deposits than the lower part of the unit; and it also includes bones in the siliciclastic deposits (Fig. 3). The highest abundance, diversity and best preservation of tracks occur at the top of inter- to supratidal carbonate beds (Figs. 7A-H and 11), although tracks are also abundant in the siliciclastic deposits (mainly the flood plain deposits; Fig. 10A-B, D) of the coastal and alluvial plain (Fig. 11) and may even preserve the impressions of slide marks (Fig. 10B-C). In the case of bones, they occur in the flood plain deposits, where they may even be articulated and/or associated (Figs. 9A and 11), and in the splay lobe deposits, where they are commonly isolated (Figs. 9-G and 11).

Toward the upper part of the unit, marine influence increased, as indicated by the presence of bioclastic, oolitic and peloidal limestone beds (which include very scarce dinosaur fossils) deposited in an inner carbonate platform (Fig. 11). This evolution would represent the record of a marine transgression as reported by Campos-Soto *et al*. (2016b). The southern sector (FA and MO sections), which was located in a more distal position and closer to the Tethys sea than the northern CE and CAS sections (Figs. 1C, 2 and 3), underwent higher marine influence. This is indicated by the increase in abundance and thickness of the bioclastic, oolitic and peloidal limestone beds toward the southern sector (FA and MO sections; Fig. 3), which contain a higher abundance of fossils indicative of normal marine salinity (such as corals, echinoderms and dasyclad and red algae; Fig. 3), but scattered dinosaur tracks.

Therefore, this study shows that the abundance and preservation of dinosaur fossils in the Villar del Arzobispo Formation are linked to the sedimentary environments in which they are recorded. In particular, the highest abundance and best preservation of dinosaur tracks occur in tidal flat carbonate beds. These tidal deposits record abundant footprints produced by herbivorous dinosaurs (mainly sauropods, stegosaurs and scarce ornithopods), which suggests that these tidal settings might have been areas of preference for feeding or keeping cool, as indicated by Cobos *et al*. (2010; 2014). In this sense, the data presented in this work are consistent with the observations reported by Lockley *et al*. (1994a), Farlow *et al*. (2012) and D´Orazi *et al*. (2016a; 2016b and references therein), who suggested that sauropod tracks seem to be common in tidal flat and other coastal deposits. This relationship has also been observed in other Upper Jurassic coastal deposits of Iberia (e.g. Lockley *et al*., 1994b; 2007; 2008; Castanera *et al*., 2014 and references therein) and other areas of Europe (e.g. Marty, 2008; Cariou *et al*., 2014; Mazin *et al*., 2016; D´Orazi *et al*., 2016a; 2016b and references therein), North America and Africa (D´Orazi *et al*., 2016a; 2016b and references therein). Moreover, further complementary research on vertebrate ichnofacies (e.g. Hunt and Lucas, 2007; Lockley, 2007), will improve the understanding of the paleoecological and paleoenvironmental setting of the dinosaurs during the Late Jurassic of the Peñagolosa sub-basin.

6. Remarks on selected larger benthic foraminifera (LBF): implications for dating the dinosaur sites of the Villar del Arzobispo Formation.

The LBF analyzed in this paper (Figs. 12 and 13) come from the uppermost levels of the Higueruelas Formation (Fig. 12A-G) and from the lower (Fig. 12H-J) and uppermost (Fig. 13A-L) parts of the Villar del Arzobispo Formation. The rest of the Villar del Arzobispo Formation may sporadically contain small agglutinated foraminifera and less frequent porcelaneous and lamellar-perforated morphotypes, that are not studied in this work. In this sense, it is important to highlight the existing difficulties on dating properly coastal and non-marine deposits and the importance of establishing reliable correlations between deep marine facies, where the stages and stage boundaries are established, with their contemporaneous shallow marine and non-marine facies.

In the uppermost levels of the Higueruelas Formation, two successive assemblages have been recognized: a lower one dominated by *Labyrinthina mirabilis, Kurnubia* gr. *palastiniensis, Pseudocyclammina lituus* and *Pseudocyclammina* sp., which are associated to few *Andersenolina* sp., *Nautiloculina oolithica*, *Molherina basiliensis* and other small benthic foraminifera; and an upper one dominated by very small *Alveosepta* Hottinger, attributed in this paper *to A. jaccardi-personata* due to the difficulties of identification in non-centered cuts. *Alveosepta* is associated to *Redmondellina* (ex-*Alveosepta*) *powersi* (Henson). Both assemblages are attributed to the Kimmeridgian (e.g. Hottinger, 1967; Pélissié *et al*., 1984; Bassoullet, 1997). This age contrasts with the ages previously assigned for this unit of Tithonian (Aurell *et al*., 1994; 2002; Mas *et al*., 2004) or Tithonian-Early Berriasian (Aurell, 1990). It should be noted that a Kimmeridgian age for the Higueruelas Formation implies that this unit may be coeval to the Torrecilla Formation, an Upper Kimmeridgian and reefal, oncolitic and oolitic unit (Fezer, 1988; Bádenas *et al*., 2008-2009), which broadly crops out in nearby areas (e.g. Bádenas *et al*., 2008-2009; Bádenas and Aurell, 2010) and has been traditionally interpreted as older than the Higueruelas Formation (e.g. Bádenas and Aurell, 2001; 2010; Bádenas *et al*., 2003; 2008-2009).

The lower part of the Villar del Arzobispo Formation contains, in its lowermost part, small *Alveosepta jaccardi-personata*, similar to those found in the uppermost part of the underlying Higueruelas Formation. Nevertheless, upward in the lower part of the unit, *A. personata* has been clearly identified. This last species was also found in the northwestern South Iberian Basin in the same stratigraphic interval of the Villar del Arzobispo Formation (Campos-Soto *et al*. 2016a). *Alveosepta* is associated with rare

Pseudocyclammina sp., *Everticyclammina* cf. *virguliana* and *Kurnubia* gr. *palastiniensis*. The presence of abundant *Alveosepta* suggests also a Kimmeridgian age for the lower part of the Villar del Arzobispo Formation (e.g. Hottinger, 1967; Septfontaine 1987; Bassoullet, 1997; Whittaker *et al*., 1998; Velic, 2007).

The middle-upper part of the unit contains, in its uppermost part, a LBF assemblage dominated by *Anchispirocyclina lusitanica* (Egger). However, the specimens from the studied samples are smaller than those of *A. lusitanica* from the type-locality (Lagosteiros beach, Cape Espichel, Portugal). The same characteristics have been observed by Hottinger (1967) in his *A. lusitanica lusitanica* from Morocco and also in the specimens from Miyares (Asturias, González-Fernández *et al*., 2014). *Anchispirocyclina lusitanica* is mainly associated with small *Choffatella* attributed to *C.* cf. *tingitana* Hottinger. Similar morphotypes have been mentioned in the Upper Jurassic facies of Asturias (NW Spain, González-Fernández *et al*., 2014). The representatives of the genera *Rectocyclammina*, *Everticyclammina, Nautiloculina* and *Andersenolina* are rare. The age of the assemblage observed in this upper part is controversial. Loeblich and Tappan (1987) reported the genus *Anchispirocyclina* from the Late Jurassic to the earliest Cretaceous, but Egger (1902) suggested a latest Jurassic age for *Dicyclina lusitanica* from the Cape Espichel (Portugal). The age proposed by Egger was retained by Hottinger (1967), who suggested a Portlandian age, by Pélissié *et al*. (1984) with a Middle-Late Portlandian age and by Bassoullet (1997) with a Tithonian age. Septfontaine *et al*., (1991) and Velic (2007) reported an *A. lusitanica* taxon-range zone in the Late Tithonian. It is interesting to mention that an earliest Cretaceous age has been used for this species by some authors in regional works after Galbrun *et al*. (1990), who reported *A. lusitanica* from the locality of Bias do Norte (Portugal) in deposits corresponding to the Chrons M18r and M18n.

In the studied unit, the dinosaur assemblages show a strong Upper Jurassic affinity, and are very similar to other dinosaur assemblages from Europe equivalent in age (Cobos *et al*., 2010; 2014), such as those reported from the Kimmeridgian-Tithonian deposits of Portugal (e.g. Mateus *et al*., 2006; Escaso *et al*., 2007; 2014; Mocho *et al*., 2017) and from the Kimmeridgian deposits of northern Spain (e.g. Lockley *et al*., 2007; Avanzini *et al*., 2010; 2012). Consequently, the data furnished by the LBF, together with the dinosaur assemblages, indicate a Kimmeridgian age for the lower part of the Villar del Arzobispo Formation and a Tithonian age for middle-upper part of the unit.

This new age assigned in this work for the Villar del Arzobispo Formation considerably differs from the Late Tithonian-Middle Berriasian age previously proposed by Aurell *et al*., (1994) and Mas *et al*. (2004). This new age also differs from the Middle Tithonian-Middle Berriasian age assigned by Aurell *et al*. (2016) to the studied deposits, which is based on data obtained in the Galve sub-basin but not in the studied area. Moreover, these authors have proposed that the deposits of the upper part of the Villar del Arzobispo Formation in the Peñagolosa sub-basin (*sensu* Cobos *et al*., 2010; 2014) are equivalent to a new lithostratigraphic unit, the Aguilar del Alfambra Formation, which they defined in the adjacent Galve sub-basin (Fig. 1B) based on the presence of an erosive unconformity between them. However, this proposal is not supported by any geological mapping, stratigraphic sections and/or biostratigraphic data of the area studied in this work. Thus, the lack of data provided by these authors from the studied area, together with the fact that: 1) the parastratotype of the Villar del Arzobispo Formation is located at the Peñagolosa sub-basin (close to Cedrillas village; Mas *et al*., 2004), 2) no erosive unconformity has been observed within the studied deposits (Figs. 2 and 3), and 3) the different age that they have attributed to the studied deposits, which is based on data not collected in the studied area, lead us to disagree with their interpretations and not accept the new lithostratigraphic divisions that Aurell *et al*. (2016) propose.

7. Conclusions

The present work clearly shows that there is a strong relationship between sedimentary facies and the distribution of dinosaur tracks and bones. Indeed, this relationship is exceptionally well represented in the Villar del Arzobispo Formation cropping out in the western Peñagolosa sub-basin, where this unit records abundant and diverse dinosaur tracks and bones in a wide variety of sedimentary paleoenvironments, ranging from shallow marine to coastal and alluvial settings, which were ideal for the vertebrate ecosystems and for the preservation of their fossils:

- The lower part of the unit was deposited in an inner carbonate platform, which episodically underwent subaerial exposure and siliciclastic inputs from the emergent areas. This environment evolved upward into a siliciclastic coastal and alluvial plain, which was crossed by fluvial channels and affected by periodic floods, giving rise to deposition of splay lobes. Progressively upward, inter- to supratidal limestone beds were interbedded with the siliciclastic coastal and alluvial plain deposits. This setting gradually evolved upward into an inner carbonate platform.

- Dinosaur tracks are most abundant, diverse and best preserved in the inter- to supratidal limestone beds, although they are also abundant in the siliciclastic deposits of the coastal and alluvial plain (mainly in the flood plain deposits). Additionally, dinosaur tracks are scarce and poorly-preserved at the top surface of shallow marine carbonates and were recorded during subaerial exposure episodes. Dinosaur bones occur both in the flood plain deposits of the coastal and alluvial plain, where they may even be articulated and/or associated, and in the splay lobe deposits, where they are generally isolated.

- The study of larger benthic foraminifera has helped significantly in redefining the age of the Villar del Arzobispo Formation and, thus, of the dinosaur fossils that it includes. The analysis of these foraminifera indicates a Kimmeridgian-Tithonian age for the Villar del Arzobispo Formation and for its dinosaur fossils, instead of the Tithonian-Berriasian ages previously assigned. A Late Jurassic age is consistent with the dinosaur assemblages present in the unit, which display a strong Upper Jurassic affinity. Moreover, the micropaleontological analysis of the uppermost levels of the underlying Higueruelas Formation suggests a Kimmeridgian age instead of the Tithonian or Tithonian-Early Berriasian ages previously assigned.

- A Late Jurassic age for the Villar del Arzobispo and Higueruelas Formations in the Peñagolosa sub-basin is consistent with the data published for the South Iberian Basin and strongly suggests the revision of the ages and stratigraphic correlations of the Upper Jurassic units deposited in nearby areas of the Iberian Basin.

Acknowledgments

This paper is dedicated to the memory of Laura Fernández Labrador, whose enthusiasm and charisma encourage us to improve and to become better persons every day. This research was funded by the Spanish projects CGL2014-52670-P, CGL2013-41295-P DINOTUR and CGL2015-69805-P of the Ministry of Economy and Competitiveness, by the "Sedimentary Basin Analysis" UCM Research Group 910429, by the Department of Education, Culture and Sport and the Department of Innovation, Research and University of the Government of Aragón, by the European Social Fund (FOCONTUR Consolidated Research Group E62), by the Instituto Aragonés de Fomento and by the Instituto de Estudios Turolenses (Diputación Provincial de Teruel). SCS is supported by a FPU predoctoral fellowship of the Spanish Ministry of Education (FPU13/02978) and PSG is supported by a postdoctoral fellowship of the Alexander von Humboldt Foundation. The authors thank reviewers Drs. M.G. Lockley and S.G. Lucas for their comments, which have greatly improved the paper. We are also thankful to Beatriz Moral, Juan Carlos Salamanca, Aitor Antón and Aida Adsuar for thin-section preparation and laboratory support, to Laura Donadeo for help with bibliography and to Valle López for help with ArcGIS. We are grateful to Dr. F. Rodríguez-Tovar for his comments about the classification of some invertebrate trace fossils.

References

Alcalá, L., Cobos, A., Royo, R., 2003. Icnitas de dinosaurio en El Castellar (Teruel). XIX Jornadas de la Sociedad Española de Paleontología, Morella (Castellón, Spain). Libro de Resúmenes 28–29.

Alcalá, L., Mampel, L., Royo-Torres, R., Cobos, A. 2014a. On small quadrupedal ornithopod tracks in Jurassic-Cretaceous transition intertidal deposits (El Castellar, Teruel, Spain). Spanish Journal of Palaeontology 29, 183-190.

Alcalá, L., Pérez-Lorente, F., Luque, L., Cobos, A., Royo-Torres, R., Mampel, L., 2014b. Dinosaur footprints in shallowing intertidal deposits of the Jurassic–Cretaceous transition in the Iberian Range (Teruel, Spain). Ichnos 2, 19-31. DOI: 10.1080/10420940.2013.873721

Allen, J.R.L. 1997. Subfossil mammalian tracks (Flandrian) in the Severn Estuary, S.W. Britain: mechanics of formation, preservation and distribution. Phil. Trans. R. Soc. Lond. 352, 481-518.

Alonso-Zarza, A.M., Wright, V.P. 2010. Palustrine carbonates, in: Alonso-Zarza, A.M., Tanner, L.H. (Eds.), Carbonates in Continental Settings: Geochemistry, Diagenesis and Applications. Developments in Sedimentology 61, Elsevier, Amsterdam, pp. 103-132. DOI: 10.1016/S0070-4571(09)06202-5.

Ataol, M. 2015. A crevasse splay induced avulsion on the Ceyhan Delta. The Journal of International Social Research 8, 675-681.

Aurell, M. 1990. El Jurásico superior de la Cordillera Ibérica Central (provincias de Zaragoza y Teruel). Análisis de Cuenca. Tesis Doctoral. Universidad de Zaragoza, Zaragoza.

Aurell, M., Mas, R., Meléndez, A., Salas, R. 1994. El tránsito Jurásico-Cretácico en la Cordillera Ibérica: relación tectónica-sedimentación y evolución paleogeográfica. Cuadernos de Geología Ibérica 18, 369-396.

Aurell, M., Meléndez, G., Olóriz, F., Bádenas, B., Caracuel, J.E., García-Ramos, J.C., Goy, A., Linares, A., Quesada, S., Robles, S., Rodríguez-Tovar, F.J., Rosales, I., Sandoval, J., Suárez de Centi, C., Tavera, J.M., Valenzuela, M. 2002. Jurassic, in: Gibbons, W., Moreno, T. (Eds.), The Geology of Spain. Geological Society, London, pp. 213-254.

Aurell, M., Ipas, J., Bádenas, B., Muñoz, A. 2012. Distribución de facies con corales y estromatopóridos en el dominio interno de una plataforma carbonatada (Titónico, Cordillera Ibérica). Geogaceta 51, 71-74.

Aurell, M. Bádenas, B., Gascá, J.M., Canudo, J.I., Liesa, C.L., Soria, A.R., Moreno-Azanza, M., Najes, L. 2016. Stratigraphy and evolution of the Galve sub-basin (Spain) in the middle Tithonian-early Barremian: Implications for the setting and age of some dinosaur fossil sites. Cretaceous Research 65, 138-162. DOI: 10.1016/j.cretres.2016.04.020

Avanzini, M., Piñuela, L., García-Ramos, J.C. 2010. First report of a Late Jurassic lizard-like footprint (Asturias, Spain). Jorunal of Iberian Geology 36, 175-180. DOI:10.5209/rev_JIGE.2010.v36.n2.5

Avanzini, M., Piñuela, L., García-Ramos, J.C. 2012. Late Jurassic footprints reveal walking kinematics of theropod dinosaurs. Lethaia 45, 238-252. DOI: 10.1111/j.1502-3931.2011.00276.x

Bádenas, B., Aurell, A. 2001. Kimmeridgian palaeogeography and basin evolution of northeastern Iberia. Palaeogeography, Palaeoclimatology, Palaeoecology 168, 291-310. DOI: 10.1016/S0031-0182(01)00204-8

Bádenas, B. Aurell, M., Rodríguez-Tovar, F.J., Pardo-Igúzquiza, E. 2003. Sequence stratigraphy and bedding rhythms of an outer ramp limestone succession (Late Kimmeridgian, Northeast Spain). Sedimentary Geology 161, 153-174. DOI: 10.1016/S0037-0738(03)00099-X

Bádenas, B., Aurell, M., Ipas, J., Espílez, E. 2008-2009. Evolución de facies y secuencias de alta frecuencia en las plataformas del final del Jurásico al suroeste de la provincia de Teruel. Teruel 92, 69-96.

Bádenas, B. Aurell, M. 2010. Facies models of a shallow-water carbonate ramp based on distribution of non-skeletal grains (Kimmeridgian, Spain). Facies 56, 89-110. DOI: 10.1007/s10347-009-0199-z

Bassoullet, J-P. 1997. Les Grands Foraminifères, in: Cariou, E., Hantzperque, P. (Coords.), Biostratigraphie du Jurassique ouest-européen et méditerranéen, Bulletin Centre Recherche Elf Exploration-Production, Mémoire 17, Pau, pp. 293-304.

Benito, M.I., Cobos, A., Mas, R., Alcalá, L., Campos-Soto, S., Fernandez, L., Quijada, E., Royo-Torres, R., Suarez-Gonzalez. P., Verdu, F. 2015. “Walking on tides”: Sedimentary controls on dinosaur tracks formation and preservation in the Barremian coastal-alluvial to tidal-flat deposits of SE Spain, W Peñagolosa subbasin, Maestrat Basin. 9th International Conference on Tidal Sedimentology, pp. 117-120 (Abstracts).

Cain, S.A., Mountney, N.P. 2009. Spatial and temporal evolution of a terminal fluvial fan system: the Permian Organ Rock Formation, South-east Utah, USA. Sedimentology 56, 1774-1800. DOI: 10.1111/j.1365-3091.2009.01057.x

Campos-Soto, S., Benito, M. I., Mas, R., Caus, E., Cobos, A., Suarez-Gonzalez, P., Quijada, I.E. 2016a. Revisiting the Late Jurassic-Early Cretaceous of the NW

South Iberian Basin: new ages and sedimentary environments. Journal of Iberian Geology 42, 69-94. DOI: 10.5209/rev_JIGE.2016.v42.n1.51920.

Campos-Soto, S., Caus, E., Bucur, I.I., Bentio, M.I., Suarez-Gonzalez, P., Quijada, I.E., Fernandez, L., Mas, R. 2016b. Registro de una transgresión marina en torno al tránsito Jurásico-Cretácico al oeste de la sub-cuenca de Peñagolosa (Teruel). Geo-Temas 16, 121-124.

Canerot, J., Cugny, P., Pardo, G., Salas, R., Villena, J. 1982. Ibérica Central-Maestrazgo, in: García, A. (Ed.), El Cretácico de España. Universidad Complutense de Madrid, Madrid, pp. 273-344.

Cariou, E., Olivier, N., Pittet, B., Mazin, J.M., Hantzpergue. 2014. Dinosaur track record on a shallow carbonate-dominated ramp (Loulle section, Late Jurassic, French Jura). Facies 60, 229-253. DOI 10.1007/s10347-013-0368-y

Castanera, D., Vila, B., Razzolini, N.L., Santos, V.F., Pascual, C., Canudo, J.L. 2014. Sauropod trackways of the Iberian Peninsula: palaeoetological and palaeoenvironmental implications. Journal of Iberian Geology 40, 49-59. DOI: 10.5209/rev_JIGE.2014.v40.n1.44087

Cobos, A., Mampel, L., Royo-Torres, R., Espílez, E., Alcalá, L. 2005. Nuevos yacimientos de icnitas de dinosaurio en Formiche Alto (Teruel). Geogaceta 38, 19-22.

Cobos, A., Royo-Torres, R., Alcalá, L., Luque, L., Aberasturi, A., 2008. Nuevos datos de las icnitas de dinosaurios en la Formación Villar del Arzobispo (Teruel). XXIV Jornadas de la Sociedad Española de Paleontología, Colunga (Asturias, Spain). Libro de Resúmenes, pp. 25–26.

Cobos, A., Royo-Torres, R., Alcalá, L., Mampel, L. 2009. Stegosaurian Dinosaurs from the Villar del Arzobispo Formation of Teruel (Spain). Tenth International Symposium on Mesozoic Ecosystems, pp. 135-136 (Abstracts).

Cobos, A., Royo-Torres, R., Luque, L., Alcala, L., Mampel, L., 2010. An Iberian stegosaurs paradise: the Villar del Arzobispo Formation (Tithonian–Berriasian) in Teruel (Spain). Palaeogeography, Palaeoclimatology, Palaeoecology 293, 223–236. DOI:10.1016/j.palaeo.2010.05.024

Cobos, A., 2011. Los dinosaurios de Teruel como recurso para el desarrollo territorial. Tesis doctoral, Univ. País Vasco. Unpublished.

Cobos, A., Alcalá, L., Mampel, L. 2012. Stegosaurian footprints from the Jurassic-Cretaceous transition in Teruel (Spain). The 11th Symposium on Mesozoic Terrestrial Ecosystems, pp. 407-409 (Abstracts).

Cobos, A., Lockley, M.G., Gascó, F., Royo-Torres, R., Alcalá, L. 2014. Megatheropods as apex predators in the typically Jurassic ecosystems of the Villar del Arzobispo Formation (Iberian Range, Spain). Palaeogeography, Palaeoclimatology, Palaeoecology 399, 31–41. DOI: 10.1016/j.palaeo.2014.02.008

Cobos, A., Royo-Torres, R., Torrente, M.A., Alcalá, L. 2015. Nuevos fósiles de dinosaurios en la Formación Villar del Arzobispo de El Castellar y Formiche Alto (Teruel, España). Geogaceta 58, 47-50.

Cobos, A., Gascó, F., Royo-Torres, R., Lockley, M.G. 2016. Dinosaur Tracks as “Four-Dimensional Phenomena” Reveal How Different Species Moved, in: Falkingham, P.L., Marty, D., Richter, A. (Eds.), Dinosaur Tracks: The Next Steps. Indiana University Press, Bloomington, pp. 244-256.

Coleman, J. M. 1976. Deltas: processes of deposition and models for exploration. Continuing Education Publication Company, Louisiana.

Coleman, J. M., Prior, D. B. 1982. Deltaic Sand Bodies. AAPG, Tulsa.

Collinson, J.D. 1996. Alluvial sediments, in: Reading, H.G. (Ed.), Sedimentary Environments: Processes, Facies and Stratigraphy, 3rd ed. Blackwell Science, Oxford, pp. 37-82.

Currie, P.J., Nadon, G.C., Lockley, M.G. 1991. Dinosaur footprints with skin impressions from the Cretaceous of Alberta and Colorado. Canadian Journal of Earth Sciences 28, 102-115. DOI: 10.1139/e91-009

Deluca, J.L., Eriksson, K.A. 1989. Controls on synchronous ephemeral- and perennial-river sedimentation in the middle sandstone member of the Triassic Chinle Formation, northeastern New Mexico, U.S.A. Sedimentary Geology 61, 155-175. DOI: 10.1016/0037-0738(89)90056-0

Demicco, R.V., Hardie, L.A. 1994. Sedimentary Structures and Early Diagenetic Features of Shallow Marine Carbonate Deposits. SEMP Atlas Series No. 1, Tulsa. DOI: 10.2110/sepmatl.01.

Díaz-Molina, M., Yébenes, A. 1987. La sedimentación litoral y continental durante el Cretácico inferior. Sinclinal de Galve, Teruel. Estudios geológicos 43(Extra), 3-21. DOI: 10.3989/egeol.8743Extra623.

Difley, R.L., Ekdale, A.A. 2002. Footprints of Utah’s Last Dinosaurs: Track Beds in the Upper Cretaceous (Maastrichtian) North Horn Formation of the Wasatch Plateau, Central Utah. Palaios 17, 327-346. DOI: 10.1669/0883-1351(2002)017<0327:FOUSLD>2.0.CO;2

D´Orazi, P., Bernardi, M., Cinquegranelli, A., Santos, V. F. D., Marty, D., Petti, F. M., Caetano, P.S., Wagensommer, A. 2016a. A review of the dinosaur track record from Jurassic and Cretaceous shallow marine carbonate depositional environments, in: Falkingham, P.L., Marty, D., Richter, A. (Eds.), Dinosaur Tracks: The Next Steps. Indiana University Press, Bloomington, pp. 381-390.

[dataset] D´Orazi, P., Bernardi, M., Cinquegranelli, A., Santos, V. F. D., Marty, D., Petti, F. M., Caetano, P.S., Wagensommer, A. 2016b. A review of the dinosaur track record from Jurassic and Cretaceous shallow marine carbonate depositional environments. Appendix. Figshare. DOI: 10.6084/m9.figshare.1348706

Dunham, R.J. 1962. Classification of carbonate rocks according to depositional texture, in: Ham, W.E. (Ed.), Classification of Carbonate Rocks. Memoir 1, AAPG, Tulsa, pp. 108- 121.

Egger, J, G. 1902. Der Bau der Orbitolinen und verwandter Formen.Abhandlungen der königlich bayerischen Akademie der Wissenschaften. Mathematisch-Physikalische Classe 21, 577-600.

Escaso, F., Ortega, F., Dantas, P., Malafaia, E., Pimentel, N.L., Pereda-Suberbiola, X., Sanz, J.L., Kullberg, J.C., Kullberg, M.C., Barriga, F. 2007. New evidence of shared dinosaur across Upper Jurassic Proto-North Atlantic: Stegosaurus from Portugal. Die Naturwissenschaften 94, 367-374. DOI: 10.1007/s00114-006-0209-8

Escaso, F., Ortega, F., Dantas, P., Malafaia, E., Silva, B., Gasulla, J.M., Mocho, P., Narváez, I., Sanz, J.L. 2014. A new dryosaurid ornithopod (Dinosauria, Ornithischia) from the Late Jurassic of Portugal. Journal of Vertebrate Paleontology, 34, 1102-1112. DOI: 10.1080/02724634.2014.849715

Ethridge, F.G. 2011. Interpretation of ancient fluvial channel deposits: review and recommendations, in: Davidson S.K., Leleu, S., North, C.P. (Eds.), From River to Rock Record. The preservation of fluvial sediments and their subsequent interpretation. SEPM Special Publication, Tulsa, pp. 9-36.

Farrel, K.M. 1987. Sedimentology and facies arquitecture of overbank deposits of the Mississippi River, False River Region, Louisiana, in: Ethridge, F.G., Flores, R.M., Harvey, M.D. (Eds.). Recent Developments in Fluvial Sedimentology. Society of Economic Paleontologists and Mineralogists, Special Publication 39, Tulsa, pp. 111-120.

Felgueroso, C., Ramírez del Pozo, J. 1971. Estratigrafía del Jurásico en la zona de Teurel-Morella (Maestrazgo). Cuadernos de Geología Ibérica 2, 439-488.

Fezer, R. 1988. Die oberjurassische karbonatische Regressionsfazies im südwestlichen Keltiberikum zwischen Griegos und Aras de Alpuente (Prov. Teruel, Cuenca, Valencia; Spanien). Arb. Inst. Geol. Paläontol. 84, 1-119.

Freytet, P., Plaziat, J.C. 1982. Continental carbonate sedimentation and pedogenesis: Late Cretaceous and Early Tertiary of Southern France. Contributions to Sedimentology 12. E. Schweizerbart´sche Verlagsbuchhandlun (Nägele u. Obermiller), Stuttgart.

Galbrun, B., Berthou, P.-Y., Moussin, C., Azéma, J. 1990. Magnétostratigraphie de la limite Jurassique-Crétacé en facies de plate-forme carbonatée: la coupe de Bias do Norte (Algarve, Portugal). Bull. Soc. Géol. France 8, 133-143.

Gatesy, S.M. 2001. Skin impressions of Triassic theropods as records of foot movement. Bulletin of the Museum of Comparative Zoology 156, 137–149.

Gautier, F. 1968. Sur la stratigraphie et les facies du Jurassique supériur et du Crétacé inérieur au Nord de Teruel (Espagne). C.R. Somm. Soc. Géol. France 2, 43-44.

Gautier, F. 1981. Hoja geológica num. 568 (Alcalá de la Selva). Mapa geológico de España E. 1:50.000. Segunda serie. IGME, Madrid.

Godoy, A., Ramírez, J.I., Olivé, A., Moissenet, E., Aznar, J.M., Aragonés, E., Aguilar, M.J., Leal, M.C., Jerez Mir, L., Adrover, R., Goy, A., Comas, M.J., Alberdi, M.T., Giner, J., Gutierrez Elorza, M., Portero, J.M., Gabaldón, V. 1983. Hoja geológica num. 567 (Teruel). Mapa geológico de España E. 1:50.000. Segunda serie. IGME, Madrid.

Godoy, A., Anadón, P., Berastegui, J., Ramírez, J.I., Olivé, A., Aguilar, M.J., Leal, M.C. García, J.C., Martín, J.M., Meléndez, A., Alvaro, M., Sole, N., Hernández, A. gabaldón, V. 1986. Hoja geológica num. 591 (Mora de Rubielos). Mapa geológico de España E. 1:50.000. Segunda serie. IGME, Madrid.

Gómez, J.J. 1979. El Jurásico en facies carbonatadas del Sector Levantino de la Cordillera Ibérica. Seminarios de Estratigrafía, Serie Monografías 4, Madrid.

Gómez, J.J., Goy, A. 1979. Las unidades litoestratigráficas del Jurásico medio y superior, en facies carbonatadas del Sector Levantino de la Cordillera Ibérica. Estudios Geológicos 35, 569- 598.

González-Fernández, B., Menéndez-Casares, E., Vicedo, V., Aramburu, C., Caus, E. 2014. New insights about the Upper Jurassic – Lower Cretaceous sedimentary successions from Asturias (NW Iberian Peninsula). Journal of Iberian Geology 40, 409-430. DOI: 10.5209/rev_JIGE.2014.v40.n3.43078

Gradstein, F.G., Ogg, J.G., Schmitz, M.D., Ogg, G.M. 2012. The Geologic Time Scale. Elsevier, Boston. DOI: 10.1016/B978-0-444-59425-9.00004-4

Grover, G., Read, J.F. 1978. Fenestral and associated vadose diagenetic fabrics of tidal flat carbonates, Middle Ordovician New Market Llimestone, Southwestern Virginia. Journal of Sedimentary Petrology 48, 453-473.

Hanley, J.H., Steidtmann, J.R. 1973. Petrology of limestone lenses in the Casper Formation, Southernmost Laramie Basin, Wyoming and Colorado. Journal of Sedimentary Petrology 43, 428-434.

Hernández, A., Godoy, A., Alvaro, M., Ramírez, J.I., Leal, M.C., Aguilar, M., Anadón, P., Moissenet, E., Meléndez, A., Gómez, J.J., Martín, J.M., García, J.C., Aramburu, C., Ortí, F., Solé, N., 1985. Hoja geológica num. 47 (Teruel). Mapa geológico de España E. 1:200.000. Primera edición. IGME, Madrid.

Hottinger, L. 1967. Foraminiferes imperforés du Mésozoique marocain, Notes et Mémoires du Service Géologique du Maroc 209. Editions du Service Geologique du Maroc, Rabat.

Hunt, A.P., Lucas, S.G. 2007. Tetrapod Ichnofacies: A New Paradigm. Ichnos 14, 59-68. DOI: 10.1080/10420940601006826

Ipas, J., Aurell, M., Bádenas, B. 2004a. Ambientes sedimentarios y secuencias en la Fm. Higueruelas (Jurásico Superior) en la Cordillera Ibérica Septentrional. Geogaceta 35, 7-10.

Ipas, J., Aurell, M., Bádenas, B. 2004b. Propuesta de correlación de las Secuencias del Titónico (Jurásico Superior) entre los sectores septentrional y oriental de la Cuenca Ibérica. Geo-Temas 6, 79-82.

Ipas, J., Aurell, M., Bádenas, B. 2005. Las unidades del tránsito Jurásico-Cretácico del Maestrazgo septentrional (NE de Teruel). Geogaceta 38, 7-10.

Ipas, J., Aurell., M., Bádenas, B., Canudo, J. I., Liesa, C., Mas, J. R., Soria, A. R. 2007. Caracterización de la Formación Villar del Arzobispo al sur de Zaragoza (Titónico, Cordillera Ibérica). Geogaceta 41, 111-114.

Laporte, L.F., Behrensmeyer, A.K. 1980. Tracks and substrate reworking by terrestrial vertebrates in Quaternary sediments of Kenya. Journal of Sedimentary Petrology 50, 1337-1346.

Lockley. M.G., Hunt, A.P. 1994. Fossil Footprints of the Dinosaur Ridge Area, A publication of the Friends of Dinosaur Ridge and the University of Colorado at

Denver Dinosaur Trackers Research Group, with the Morrison Museum of Natural History.

Lockley, M.G., Meyer, C.A., Hunt, A.P., Lucas, S.G. 1994a. The distribution of sauropod tracks and trackmakers. Gaia 10, 233-248.

Lockley, M.G., Meyer, C.A., Santos, V.F.D. 1994b. Trackway evidence for a herd of juvenile sauropods from the Late Jurassic of Portugal. Gaia 10, 27-35.

Lockley, M.G. 2003. Fossil footprints of the Dinosaur Ridge and Fossil Trace areas. A publication of the Friends of Dinosaur Ridge, Morrison Colorado.

Lockley, M. 2007. A Tale of Two Ichnologies: The Different Goals and Potentials of Invertebrate and Vertebrate (Tetrapod) Ichnotaxonomy and How They Relate to Ichnofacies Analysis. Ichnos 14, 39-57. DOI: 10.1080/10420940601006818

Lockley, M.G., Lire, J., García-Ramos, J.C., Pinuela, L., Avanzini, M. 2007. Shrinking the World's Largest Dinosaur Tracks: Observations on the Ichnotaxonomy of Gigantosauropus asturiensis and Hispanosauropus hauboldi from the Upper Jurassic of Asturias, Spain. Ichnos 14, 247-255. DOI: 10.1080/10420940601050048

Lockley, M.G., Garcia-Ramos, J.C., Lires, J., Pinuela, L. and Avanzini, M. 2008. A review of vertebrate track assemblages from the Late Jurassic of Asturias, Spain with comparative notes on coeval ichnofaunas from the western USA: implications for faunal diversity in association with siliciclastic facies assemblages. Oryctos 8, 53-70.

Loeblich, A., Tappan, H. 1987. Foraminiferal Genera and Their Classification. Van Nostrand Reinhold Company, New York, 2 vol.

Luque, L., Cobos, A., Royo-Torres, R., Espílez, E., Alcalá, L. 2005. Caracterización de los depósitos sedimentarios con dinosaurios de Riodeva (Teruel). Geogaceta 38, 27-30.

MacEachern, J. A., Bann, K.L., Pemberton, S. G., Gringras, M.K. 2007. The ichnofacies paradigm: high-resolution paleoenvironmental interpretation of the rock record, in: MacEachern, J.A., Bann, K.L., Gingras, M.K., Pemberton, S.G. (Eds.), Applied Ichnology, SEPM Short Course Notes 52, Tulsa, pp. 27–64. DOI: 10.2110/pec.07.52.0027.

Martín-Closas, C. 1989. Els carofits del Cretaci inferior de les conques periferiques del Bloc de l'Ebre, Tesis Doctoral ed, Universidad de Barcelona, Barcelona. Unpublished

Marty, D. 2008. Sedimentology, taphonomy, and ichnology of Late Jurassic dinosaur tracks from the Jura carbonate platform (Chevenez-Combe Ronde tracksite, NW Switzerland): insights into the tidal-flat palaeoenvironment and dinosaur diversity, locomotion, and palaeoecology. Ph.D. Thesis University of Fribourg (Switzerland), GeoFocus, 21.

Marty, D., Strasser, A., Meyer, C.A. 2009. Formation and Taphonomy of Human Footprints in Microbial Mats of Present-Day Tidal-flat Environments: Implications for the Study of Fossil Footprints. Ichnos 16, 127-142. DOI: 10.1080/10420940802471027

Mas, R., Alonso, A. 1981. Trabajo estratigráfico, sedimentológico y paleogeográfico de las facies Purbeck, Weald y Utrillas en el sector suroriental de la Cordillera Ibérica. Hoja geológicas num. 55 (Lliria) y 43 (Valencia) del Mapa Geológico de España E. 1:200.000. Segunda serie. IGME, Madrid. Unpublished.

Mas, R., Alonso, A., Meléndez, N. 1984. La formación Villar del Arzobispo: un ejemplo de llanuras de mareas siliciclásticas asociadas a plataformas carbonatadas. Jurasico terminal. (NW de Valencia y E de Cuenca). Publicaciones de Geología 20, 175-188.

Mas, R., García, A., Salas, R., Meléndez, A., Alonso, A., Aurell, M., Bádenas, B., Benito, M.I., Carenas, J.F., García-Hidalgo, J., Gil, J., Segura, M. 2004. Segunda fase de rifting: Jurásico Superior-Cretácico Inferior, in: Vera, J.A. (Ed.), Geología de España. SGE-IGME, Madrid, pp. 503-510.

Mateus, O., Walen, A. & Antunes, M.T. 2006. The large theropods fauna of the Lorurinhã Formation (Portugal) and its similarity to the Morrison Formation, with a description of a new species of Allosaurus. New Mexico Museum of Natural History and Science 36, 223-231.

Mazin, J.M., Hantzpergue, P., Pouech, J. 2016. The dinosaur tracksite of Loulle (early Kimmeridgian; Jura, France). Geobios 49, 211-228. DOI: 10.1016/j.geobios.2016.01.018

McKie, T. 2011. Architecture and behavior of dryland fluvial reservoirs, Triassic Skagerrak Formation, Central North Sea, in: Davidson S.K., Leleu, S., North, C.P. (Eds.), From River to Rock Record. The preservation of fluvial sediments and their subsequent interpretation. SEPM Special Publication, Tulsa, pp. 189-214.

Meléndez, A., Pardo, G., Pendón, J.G., Villena, J. 1979. Las facies terminales del Jurásico en el sector central de la Cordillera Ibérica. Cuadernos de Geología 10, 137-148.

Miall, A.D. 1996. The Geology of Fluvial Deposits. Springer, Berlin.

Mocho, P., Royo-Torres, R. Malafaia, E. Escaso, F. Ortega, F. 2017. Sauropod tooth morphotypes from the Upper Jurassic of the Lusitanian Basin (Portugal). Papers in Palaeontology, 1-37. DOI: 10.1002/spp2.1075

Moissenet, E., Gautier, E. 1971. La région de Rubielos de Mora (Province de Teruel, Chaînes Ibériques orientales). Contribution à l'étude géologique et morphologique. Mélanges de la Casa de Velázquez 7, 5-34. DOI: 10.3406/casa.1971.1033

Mutti, E., Davoli, G., Tinterri, R., Zavala, R. 1996. The Importance of Ancient Fluvio-Deltaic Systems Dominated by Catastrophic Flooding in Tectonically Active Basins. Memorie di Scienze Geologiche 8, 233-291.

Nagy, Z.R., Somerville, I.D. Gregg, J.M., Becker, S.P., Shelton, K.L. 2005. Lower Carboniferous peritidal carbonates and associated evaporates adjacent to the Leinster Massif, southeast Irish Midlands. Geological Journal 40, 173-192. DOI: 10.1002/gj.999

Pélissié, T., Peybernés, B., Rey, J. 1984. Les grands foraminifères benthiques du Jurassique moyen/supérieur du sud-ouest de la France (Aquitaine, Causses, Pyrénées). Intérêt biostratigraphique, paléoécologique et paléobiogógraphique. Benthos 83, 479-489.

Plink-Bjorklund, P. 2015. Morphodynamics of rivers strongly affected by monsoon precipitation: Review of depositional style and forcing factors. Sedimentary Geology 323, 110-147. DOI: 10.1016/j.sedgeo.2015.04.004.

Quijada, I.E., Suarez-Gonzalez, P., Benito, M.I., Mas, R. 2013. New insights on stratigraphy and sedimentology of the Oncala Group (eastern Cameros Basin): implications for the paleogeographic reconstruction of NE Iberia at Berriasian times. journal of Iberian Geology 39, 313-334. DOI: 10.5209/rev_JIGE.2013.v39.n2.42503

Quijada, I.E., Suarez-Gonzalez, P., Benito, M.I., Mas, R. 2016. Tidal versus continental sandy-muddy flat deposits: evidence from the Oncala Group (Early Cretaceous, N Spain), in: Tessier, B., Reynaud, J.Y. (Eds.), Contributions to Modern and Ancient Tidal Sedimentology: Proceedings of the Tidalites 2012 conference. John Wiley & Sons, Ltd, Chichester, pp. 113-159. DOI: 10.1002/9781119218395.ch8

Razzolini, N.L., Vila, B., Castanera, D., Falkingham, P.L., Barco, J.L., Canudo, J.I., Manning, P.L., Galobart, A. 2016. Intra-Trackway Morphological Variations Due to Substrate Consistency: The El Frontal Dinosaur Tracksite (Lower Cretaceous, Spain). PLoS One 9, 1-14. DOI: 10.1371/journal.pone.0093708

Reineck, H.-E, Singh, I. B. 1973. Depositional Sedimentary Environments With Reference to Terrigenous Clastics, 2nd ed. Sringer-Verlag, Berlin.

Royo-Torres, R., Upchurch, P., Mannion, P.D., Mas, R., Cobos, A., Gascó, F., Alcalá, L., Sanz, J.L. 2014. The anatomy, phylogenetic relationships, and stratigraphic position of the Tithonian–Berriasian Spanish sauropod dinosaur Aragosaurus ischiaticus. Zoological Journal of the Linnean Society 171, 623–655. DOI: 10.1111/zoj.12144

Santisteban, C., Santos-Cubedo, A. 2010a. Relación entre playas aterrazadas y cauces encajados, en depósitos deltaicos de la Formación Villar del Arzobispo (Cuenca Íbero-Levantina), in: Ruiz-Omeñaca, J.I., Piñuela, L., García-Ramos, J.C. (Eds.), Comunicaciones del V Congreso del Jurásico de España. Museo del Jurásico de Asturias (MUJA), Colunga, 8-11 de septiembre de 2010. Museo del Jurásico de Asturias, Colunga, pp. 135-141.

Santisteban, C., Santos-Cubedo, A. 2010b. Patrones de variación de facies en relación con regresiones forzadas en los depósitos de la Formación Villar del Arzobispo (Cuenca Íbero-Levantina), in: Ruiz-Omeñaca, J.I., Piñuela, L., García-Ramos, J.C. (Eds.), Comunicaciones del V Congreso del Jurásico de España. Museo del

Jurásico de Asturias (MUJA), Colunga, 8-11 de septiembre de 2010. Museo del Jurásico de Asturias, Colunga, pp. 142-148.

Santos, V.F., Capallez, P.M., Rodrigues, N.P.C. 2013. Dinosaur footprints from the Lower Cretaceous of the Algarve Basin (Portugal): New data on the ornithopod palaeoecology and palaeobiogeography of the Iberian Peninsula. Cretaceous Research 40, 158-169. DOI: 10.1016/j.cretres.2012.07.001

Salas, R. 1987. El Malm i el Cretaci inferior entre el Massís de Garraf i la Serra D´Espada. Anàlisi de conca. Tesis Doctoral. Universitat de Barcelona, Barcelona.

Salas, R., Guimerà, J. 1996. Rasgos estructurales principales de la cuenca cretácica inferior del Maestrazgo (Cordillera Ibérica oriental). Geogaceta 20, 1704-1706.

Salas, R., Guimerà, J. 1997. Estructura y estratigrafía secuencial de la cuenca del Maestrazgo durante la etapa de rift jurásica superior - cretácica inferior (Cordillera Ibérica oriental). Boletín Geológico y Minero 108, 393-402.

Salas, R., Guimerà, J., Mas, R., Martin-Closas, C., Melendez, A., Alonso, A. 2001. Evolution of the Mesozoic Central Iberian Rift System and its Cainozoic inversion (Iberian chain), in: Cavazza, W., Roberston, A.H.F.R., Ziegler P. (Eds.), Peri-Tethyan Rift/Wrech basins and Passive Margins. Mem. Musee National Histoire Naturelle, Paris, pp. 145-185.

Shinn, E.A. 1983a. Tidal Flat, in: Scholle, P.A., Bebout, D.G., Moore, C.H. (Eds.), Carbonate depositional environments. Memoir 33, AAPG, Tulsa, pp. 171-210.

Shinn, E.A. 1983b. Birdseyes, fenestrae, shrinkage pores, and loferites: a reevaluation. Journal of Sedimentary Research 53, 619-628.

Septfontaine, M. 1987. Vers une classification évolutive des Lituolidés (Foraminifperes) Jurasiques en Milieu de Plate-forme Carbonatée. Revue de Paléobiologie 2 (Benthos´86), 229-256.

Septfontaine, M., Arnaud-Vanneau, A., Bassoullet,J.P., Gušić, I., Ramalho, M., Velić, I. 1991. Les Foraminifères imperforés des plate-formes carbonatées jurassiques: état des connaissances et perspectives d'avenir. Bulletin Societé Vaud Sciènces Naturelles 80, 255–277.

Suarez-Gonzalez, P. Quijada, I.E., Benito, M.I., Mas, R. 2013. Eustatic versus tectonic control in an intraplate rift basin (Leza Fm, Cameros Basin). Chronostratigraphic and paleogeographic implications for the Aptian of Iberia. Journal of Iberian Geology 39, 285-312. DOI: 10.5209/rev_JIGE.2013.v39.n2.42502

Suarez-Gonzalez, P. Quijada, I.E., Benito, M.I., Mas, R. 2015. Sedimentology of Ancient Coastal Wetlands: Insights From A Cretaceous Multifaceted Depositional System. Journal of Sedimentary Research 85, 95-117. DOI: 10.2110/jsr.2015.07

Tebbutt, G.E., Conley, C.D., Boyd, D.W. 1965. Lithogenesis of a distinctive carbonate rock fabric. Rocky Mountain Geology 4, 1-13.

Turner, B.R. 1986. Tectonic and climatic controls on continental depositional facies in the Karoo Basin of Northern Natal, South Africa. Sedimentary Geology 46, 231-257. DOI: 10.1016/0037-0738(86)90061-8

Turner, B.R., Tester, G.N. 2006. The Table Rock Sandstone: A fluvial, friction-dominated lobate mouth bar sandbody in the Westfalian B Coal Measures, NE England. Sedimentary Geology 190, 97-119. DOI:10.1016/j.sedgeo.2006.05.007

Velic, I. 2007. Stratigraphy and Palaeobiogeography of Mesozoic Benthic Foraminifera of the Karst Dinarides (SE Europe). Gelogia Croatica 60, 1-113.

Whittaker, J., Wynn Jones, B., Banner, F. 1998. Key Mesozoic Benthic Foraminifera of the Middle East. The Natural History Museum, London.

Zuffa, G.G. 1980. Hybrid arenites: their composition and classification. Journal of Sedimentary Research 50, 21-29. DOI: 10.1306/212F7950-2B24-11D7-8648000102C1865D

Figure captions

Fig.1. A) Location of the studied area in the Mesozoic Iberian Extensional System (modified from Mas *et al*., 2004). B) Structural map of the Maestrazgo Basin during the Late Jurassic-Early Cretaceous (modified from Salas and Guimerà, 1996; 1997; Salas *et al*., 2001). The studied area corresponds to the western Peñagolosa sub-basin (red square). C) Paleogeographic evolution of eastern Iberia during the Late Jurassic-Early Cretaceous times (modified from Mas *et al*., 2004 according to data published by Quijada *et al.*, 2013).

Fig. 2. Geological maps of the western Peñagolosa sub-basin. Geographic latitude and longitude coordinates and Universal Transverse Mercator (UTM) coordinates are indicated in blue and black colors, respectively, at the margins of the maps (Coordinate system: Datum ETRS89, projection UTM zone 30N). A) Synthetic geological map of the studied area, indicating the location of the stratigraphic sections: Cedrillas section (CE), El Castellar section (CAS), Formiche Alto section (FA) and Mora de Rubielos section (MO). The map also shows the location of the main dinosaur sites of the Villar del Arzobispo Formation and the detailed mapping of the bioclastic, oolitic and peloidal limestone beds (dark blue lines) and the mudstone and peloidal limestone beds (light blue lines) of this unit. Location of Fig. 2B is outlined in dotted red line. B) Detailed geological map of the El Castellar area including the dinosaur sites of the Villar del Arzobispo Formation (see Fig. 2A for legend).

Fig. 3. Stratigraphic sections of the Villar del Arzobispo Formation performed in the studied area (Cedrillas section, CE, El Castellar section, CAS, Formiche Alto section, FA, Mora de Rubielos section, MO), the legend and a simplified geological map of the studied area showing their location. The main fossil remains observed in the carbonate beds are shown at the right part of each section. The stratigraphic position of the

dinosaur sites of the Villar del Arzobispo Formation is indicated in red color to the right of each section. The dinosaur sites, which were not observed along the stratigraphic sections, have been correlated into the sections and their inferred stratigraphic position is indicated with a discontinuous line and in italics to the right of each section.

Fig. 4. A) Chrono-lithostratigraphic diagram for the Peñagolosa sub-basin (data obtained from Salas *et al*., 2001; Mas *et al*., 2004). The studied unit is the Villar del Arzobispo Formation, which is highlighted in red color. B-C) Kimmeridgian to Valanginian chronostratigraphy (modified from Gradstein *et al*., 2012), showing: B) in orange color, the Boreal regional stages used before the Tithonian was formally adopted as a stage by the International Commission on Stratigraphy in 1990 (Gradstein *et al*., 2012); C) in blue color, the Stages of the Standard Chronostratigraphy (Gradstein *et al*., 2012). The right part of diagram (B) and the left part of diagram (C) show the ages assigned to the Villar del Arzobispo (VILL Fm) and Higueruelas (HIG Fm) Formations in the Peñagolosa sub-basin by different authors and in regional works by Aurell *et al*., (1994) and Mas *et al*. (2004). It is important to highlight that prior to their formal definition (Higueruelas Formation in 1979 by Gómez 1979; Gómez and Goy, 1979; Villar del Arzobispo Formation in 1984 by Mas *et al*., 1984), the Higueruelas Formation (HIG) was referred to as Kimmeridgian (e.g. Gautier, 1968) and the Villar del Arzobispo Formation (VILL) to as Portlandian or Upper Kimmeridgian-Portlandian (e.g. Gautier, 1968; Felgueroso and Ramírez del Pozo, 1971, respectively). The ages proposed in this work for the Villar del Arzobispo and Higueruelas Formations are highlighted in red color in diagram C.

Fig. 5. General views of the Villar del Arzobispo Formation. A-B) Lower part of the unit: A) General view of the deposits of the lower part of the Villar del Arzobispo Formation (next to Cedrillas village), which consist on alternating bioclastic, oolitic and

peloidal limestone beds (dark blue lines), siliciclastic mudstone (red lines), non-channelized bodies (yellow lines and arrows), minor channelized sandstone and conglomerate bodies and marl. B) Outcrop detail of the lower part of the Villar del Arzobispo Formation (next to Cedrillas village) made up of alternating bioclastic, oolitic and peloidal limestone beds (dark blue arrow), siliciclastic mudstone (red arrows) and non-channelized sandstone (yellow arrow). C-E) Middle-upper part of the unit: C) Panoramic view of the middle-upper part of the Villar del Arzobispo Formation in the north of the studied area (next to Cedrillas village), showing: 1) a middle siliciclastic part formed by siliciclastic mudstone (red arrow), non-channelized sandstone bodies, and channelized sandstone and conglomerate bodies (yellow arrows); 2) an upper siliciclastic and carbonate part composed of siliciclastic mudstone (red arrows) alternating with mudstone and peloidal limestone (light blue arrows). D) Field photograph of the upper part of the unit next to El Castellar village. Mudstone and peloidal limestone beds (light blue lines) are interbedded with siliciclastic mudstone (red lines) and non-channelized sandstone bodies (yellow arrows and lines). E) Field photograph of the uppermost part of the unit next to Cabra de Mora village showing bioclastic, oolitic and peloidal limestone beds (dark blue arrows and lines) interbedded with non-channelized sandstone bodies (yellow arrows and lines) and siliciclastic mudstone (red lines).

Fig. 6. Carbonate deposits of the Villar del Arzobispo Formation. A-F) Bioclastic, oolitic and peloidal limestone: A) Schematic log of the bioclastic, oolitic and peloidal limestone (see Fig. 3 for legend). B) Field photograph of the general appearance of this facies next to Mora de Rubielos village. C) Transmitted light (TL) micrograph of the carbonate deposits, made up of well-sorted ooids, peloids and bioclasts. D) Field photograph of a limestone bed showing an accumulation of poorly-sorted bioclasts

(mainly ostreids). E) TL micrograph of poorly-sorted bioclastic, oolitic and peloidal limestone. F) Field photograph of the top surface of a limestone bed displaying a *Rhizocorallium*-like trace. Coin diameter: 23,25 mm. G-M) Mudstone and peloidal limestone: G) Schematic log of the mudstone and peloidal limestone (see Fig. 3 for legend). H) Field photograph of the general appearance of these facies next to El Castellar village. I) Outcrop detail of alternating millimeter- to centimeter-thick mudstone and peloidal layers. Coin diameter: 23,25 mm. J) TL micrograph of the mudstone deposits, showing bioturbation filled by fecal pellets (yellow arrow) and fenestral porosity (white arrows). K) TL micrograph of the peloidal packstone-grainstone deposits formed by fecal pellets, quartz grains and scarce foraminifers (white arrows). L) Outcrop detail of a limestone bed displaying dark-grey and light-grey patches, both of them showing millimetric-sized burrows. M) Field photograph of desiccation cracks observed at the top surface of a limestone bed. Yellow scale = 20 cm.

Fig. 7. Dinosaur tracks observed in carbonate beds. A-H) Tracks at the top surface of mudstone and peloidal limestone beds: A) Ornithopod track from Masía de la Cañada site (FA-6) next to Formiche Alto village (Cobos *et al*., 2015), showing a well-defined shape, vertical walls and no displacement rim. B) *Iberosauripus* track from El Castellar site (CT-1) next to El Castellar village (Cobos *et al*., 2014) showing a moderately to well-defined shape and displaying claw marks (red arrows) and pads impressions (white arrows). C-D) Sauropod tracks from (C) El Molino site (FB-1) next to Formiche Bajo village (Cobos *et al*., 2005) and (D) El Pozo site (CT-2) next to El Castellar village (Alcalá *et al*., 2014b), characterized by moderately- to well-defined shapes and large, wide, prominent and well-defined displacement rims (white arrows). E) Camino El Berzal site (CT-3) next to El Castellar village, which includes 55 tracks including a theropod trackway and some of the largest sauropods tracks of the Iberian Peninsula

(Alcalá *et al*. 2014b; Cobos *et al*., 2014). Footprints show moderately-defined shapes and prominent, well-defined displacement rims. F) Sauropod tracks from El Pozo site (CT-2; Alcalá *et al*., 2014b). These footprints are shallow, show moderately- to poorly-defined shapes and contoured, wide and poorly-defined displacement rims (white arrow). G) *Deltapodus* pes from El Castellar site (CT-1, next to El Castellar village), displaying poorly-defined outlines (white arrows). H) Very poorly-preserved and very shallow track (white arrow) from La Curva site (CD-4) next to Cedrillas village, which shows poorly-defined outlines. I) Tracks preserved as natural casts observed at the base of mudstone and peloidal limestone (white arrows; CD-6 site, next to Cedrillas village). The infillings penetrate in the underlying reddish siliciclastic mudstone, which display edaphic features (root traces). J) Poorly-preserved tracks (CT-68 site, next to El Castellar village) at the top of bioclastic, oolitic and peloidal limestone (white arrows). K) Natural cast (MR-10 site, next to Mora de Rubielos village) observed at the base of bioclastic, oolitic and peloidal limestone (white arrows), which penetrates in the underlying grayish siliciclastic mudstone.

Fig. 8. Siliciclastic deposits of the Villar del Arzobispo Formation. A-C) Siliciclastic mudstone deposits: A) Schematic log of siliciclastic mudstone deposits (see Fig. 3 for legend). B-C) Field photograph of reddish siliciclastic mudstone displaying root traces (white arrow in C) next to Formiche Alto and Cedrillas villages (B and C, respectively). D-H) Non-channelized sandstone bodies: D, F-G) Schematic logs of non-channelized sandstone bodies (see Fig. 3 for legend). E) Field photograph of a coarsening- and thickening-upward non-channelized sandstone body (next to El Castellar village). H) Field photograph next to Cedrillas village of a non-channelized sandstone body displaying flat bases, convex tops (white arrows) and limited lateral continuity. I-K) Channelized sandstone and conglomerate bodies: I) Schematic log of channelized

sandstone and conglomerate bodies (see Fig. 3 for legend). J) Field photograph next to Cedrillas village of a channelized bed displaying erosive base (yellow dotted line). K) Outcrop detail of conglomerate composed of carbonate and muddy soft pebbles.

Fig. 9. Dinosaur bones observed in the siliciclastic deposits of the Villar del Arzobispo Formation. A-C) Bones observed in siliciclastic mudstone deposits. A) Associated sauropod fossils (white dotted lines) from La Tejería site (CT-30) next to El Castellar village. B-C) Some bones from (B) CT-45 site and (C) CT-47 site next to El Castellar village. D-F) Bone remains dispersed within non-channelized sandstone bodies from CT-61 site next to El Castellar village. G) Diplodocoidea caudal centrum found *ex situ* from Los Canales site (CT-60) next to El Castellar village (Cobos *et al*., 2015).

Fig. 10. Tracks in non-channelized sandstone bodies. A-B) Natural casts observed at the base of non-channelized sandstone bodies. A) Natural casts from La Carrasca site (CT-62) next to El Castellar village (white arrows), which penetrate in the underlying siliciclastic mudstone interbedded with sandstone. B) Natural cast from site FA-7 next to Formiche Alto village. The infilling shows vertical and parallel striations ("4D track"; white arrow) and penetrates in the underlying deposit made up of an alternation of siliciclastic mudstone and sandstone layers. Note how the underlying layers are deformed in the contact with the infilling (red arrows). C) Detail of the striations. D) Tracks from site FA-8 next to Formiche Alto village (white arrows), which penetrate in the underlying siliciclastic mudstone. E-F) *Ex situ* dinosaur tracks from (E) CT-57 and (F) CT-64 sites next to El Castellar village (theropod and stegosaur trackmakers, respectively). G-I) Tracks observed at the top of non-channelized sandstone beds in section view (G-H) and in plant view (I). G) Outcrop detail next to Cedrillas village of an infilling made up of sandstone (site CD-8). Note the deformation produced in the underneath sandstone layers (red arrow). H) Outcrop detail of an infilling made up of

siliciclastic mudstone (site CT-61 next to El Castellar village), which deforms the underneath sandy layers (red arrows). The sandstone bed is overlaid by a thin layer of siliciclastic mudstone (white arrow). I) Sauropod? manus from CD-1 site next to Cedrillas village.

Fig. 11. Idealized reconstruction of the shallow marine to coastal and alluvial depositional paleoenvironments, inhabited by dinosaurs, of the Villar del Arzobispo Formation.

Fig. 12. Larger benthic foraminifera of (A-G) the upper part of the Higueruelas Formation and (H-J) the lower part of the Villar del Arzobispo Formation. A) *Labyrinthina mirabilis* Weynschenk, 1951. Subequatorial slightly oblique section showing the early planispiral arrangement of chambers becoming uncoiled in the adult stage. B-form? (sample CAS019). B-D) *Redmondellina powersi* (Redmond), 1964, showing the beams and rafters of the exoskeleton prolonging to the previous septum in the median part of the shell. B) Tangential-oblique section, B-form (sample CE032). C) Subequatorial slightly oblique section, A-form (sample CE033). D) Axial section, B-form (sample CE032). E) *Kurnubia* gr. *palastiniensis* Henson, 1948. Subaxial section (sample CAS019). F) *Pseudocyclammina lituus* (Yokoyama), 1890. Axial non-centered section of a juvenile specimen (CAS019). G) *Pseudocyclammina* sp. Two successive chambers of large *Pseudocyclammina* (sample CAS019). H-J) *Alveosepta personata* (Tobler), 1928, showing the beams and rafters of the exoskeleton and the structured septa (sample CAS045). Note the empty chambers compared with *Redmondellina powersi*. Scale bar: 0.2 mm.

Fig. 13. Larger benthic foraminifera of the upper part of the Villar del Arzobispo Formation. A-E) *Anchispirocyclina lusitanica* (Egger), 1902, showing the planispiral to

peneropliform chambers with the characteristic fine reticular subepidermal exoskeleton formed by short beams and rafters and the pillars as the endoskeleton elements. A-B, D-E) A-forms. C) B-form. A) Equatorial section (sample MO-1A). B) Centered oblique section near the equatorial (sample MO-1B). C) Tangential-oblique section (sample MO-1B). D) Axial section (sample MO-1B). E) Equatorial section of a small specimen (sample CE117). F, H-I) *Choffatella* cf. *tingitana* Hottinger, 1967 (sample MO1-D). F) Slightly oblique equatorial section showing the fine reticular subepidermal exoskeleton similar to *Anchispirocyclina* and the foramina piercing the septa. H) Axial section. I) Subaxial section. G) *Rectocyclammina* cf. *chouberti* Hottinger, 1967, almost an axial section showing the reticular subepidermal exoskeleton and the central position of the foramen (sample CE-135). J-L) *Everticyclammina* cf. *virguliana* (Koechlin), 1942, showing the alveolar exoskeleton. J-K) Almost equatorial sections (from samples CE116 and CE117, respectively). L) Oblique section (sample CE116). Scale bar in all sections: 0.2 mm.

Table 1. Main dinosaur sites of the Villar del Arzobispo Formation in the Peñagolosa sub-basin.

Fig. 1

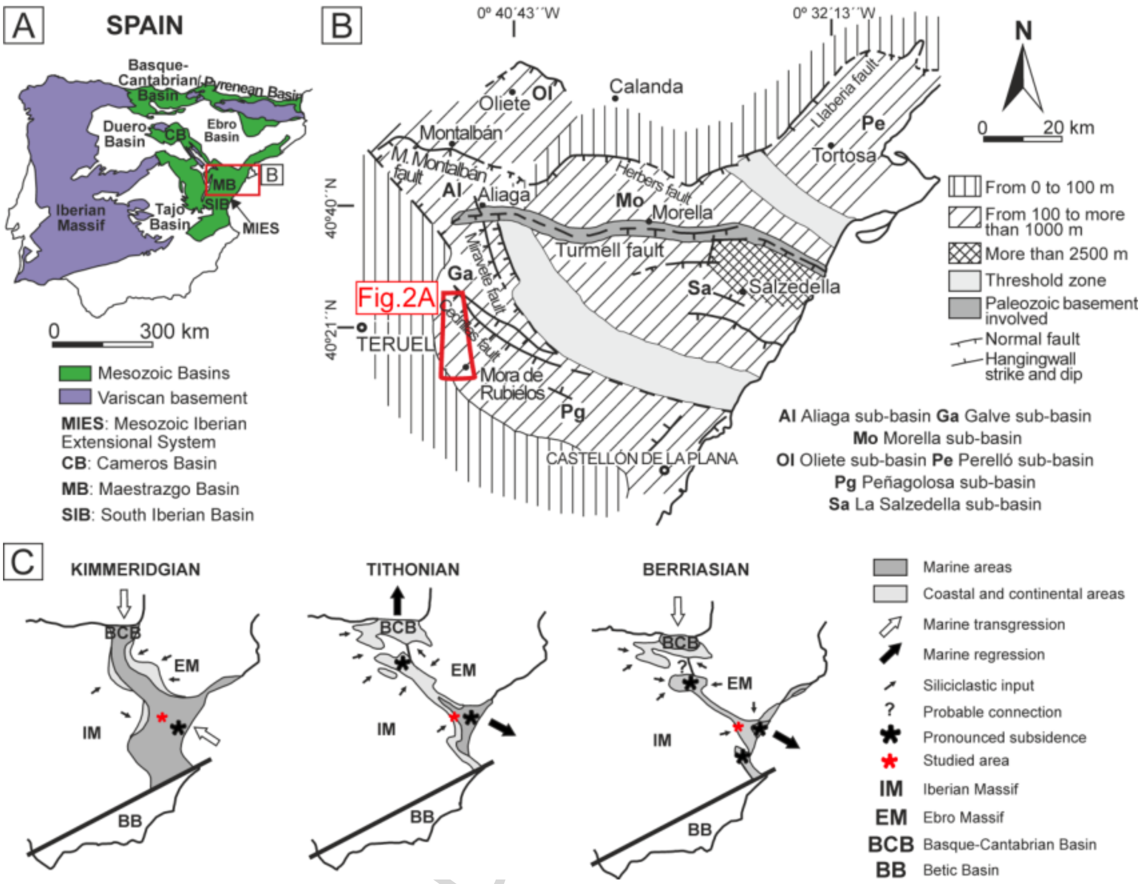
A
SPAIN
Basque-Cantabrian Basin
Pyrenean Basin
Duero Basin
CB
Ebro Basin
MB
B
Iberian Massif
Tajo Basin
SIB
MIES
0 300 km
Mesozoic Basins
Variscan basement
MIES: Mesozoic Iberian Extensional System
CB: Cameros Basin
MB: Maestrazgo Basin
SIB: South Iberian Basin
B
0° 40´43´´W
0° 32´13´´W
Ol
Oliete
Calanda
Montalbán
M. Montalbán fault
Al
Aliaga
Herbers fault
Mo
Morella
Llaberia fault
Pe
Tortosa
40°40´´N
Turmell fault
Ga
Miravete fault
Sa
Salzedella
Fig.2A
40°21´´N
TERUEL
Mora de Rubielos
Pg
CASTELLÓN DE LA PLANA
N
0 20 km
From 0 to 100 m
From 100 to more than 1000 m
More than 2500 m
Threshold zone
Paleozoic basement involved
Normal fault
Hangingwall strike and dip
Al Aliaga sub-basin Ga Galve sub-basin
Mo Morella sub-basin
Ol Oliete sub-basin Pe Perelló sub-basin
Pg Peñagolosa sub-basin
Sa La Salzedella sub-basin
C
KIMMERIDGIAN
TITHONIAN
BERRIASIAN
BCB
EM
IM
BB
?
Marine areas
Coastal and continental areas
Marine transgression
Marine regression
Siliciclastic input
Probable connection
Pronounced subsidence
Studied area
IM Iberian Massif
EM Ebro Massif
BCB Basque-Cantabrian Basin
BB Betic Basin

Fig. 2

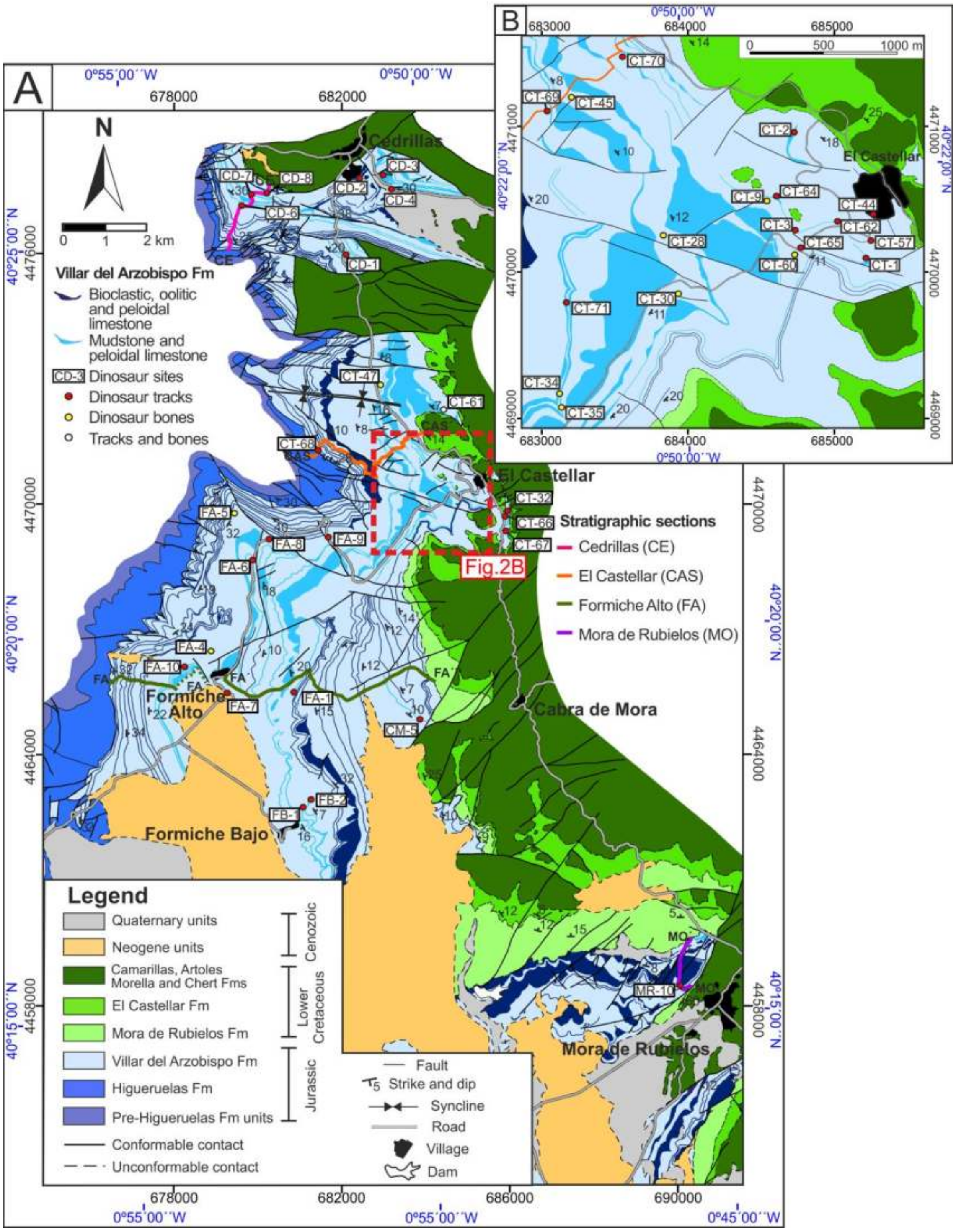

A
B
Fig.2B
Villar del Arzobispo Fm
Bioclastic, oolitic and peloidal limestone
Mudstone and peloidal limestone
CD-3 Dinosaur sites
Dinosaur tracks
Dinosaur bones
Tracks and bones
Stratigraphic sections
Cedrillas (CE)
El Castellar (CAS)
Formiche Alto (FA)
Mora de Rubielos (MO)
Legend
Quaternary units
Neogene units
Camarillas, Artoles Morella and Chert Fms
El Castellar Fm
Mora de Rubielos Fm
Villar del Arzobispo Fm
Higueruelas Fm
Pre-Higueruelas Fm units
Conformable contact
Unconformable contact
Cenozoic
Lower Cretaceous
Jurassic
Fault
Strike and dip
Syncline
Road
Village
Dam
Cedrillas
El Castellar
Formiche Alto
Formiche Bajo
Cabra de Mora
Mora de Rubielos
0 1 2 km
0 500 1000 m

Fig. 3

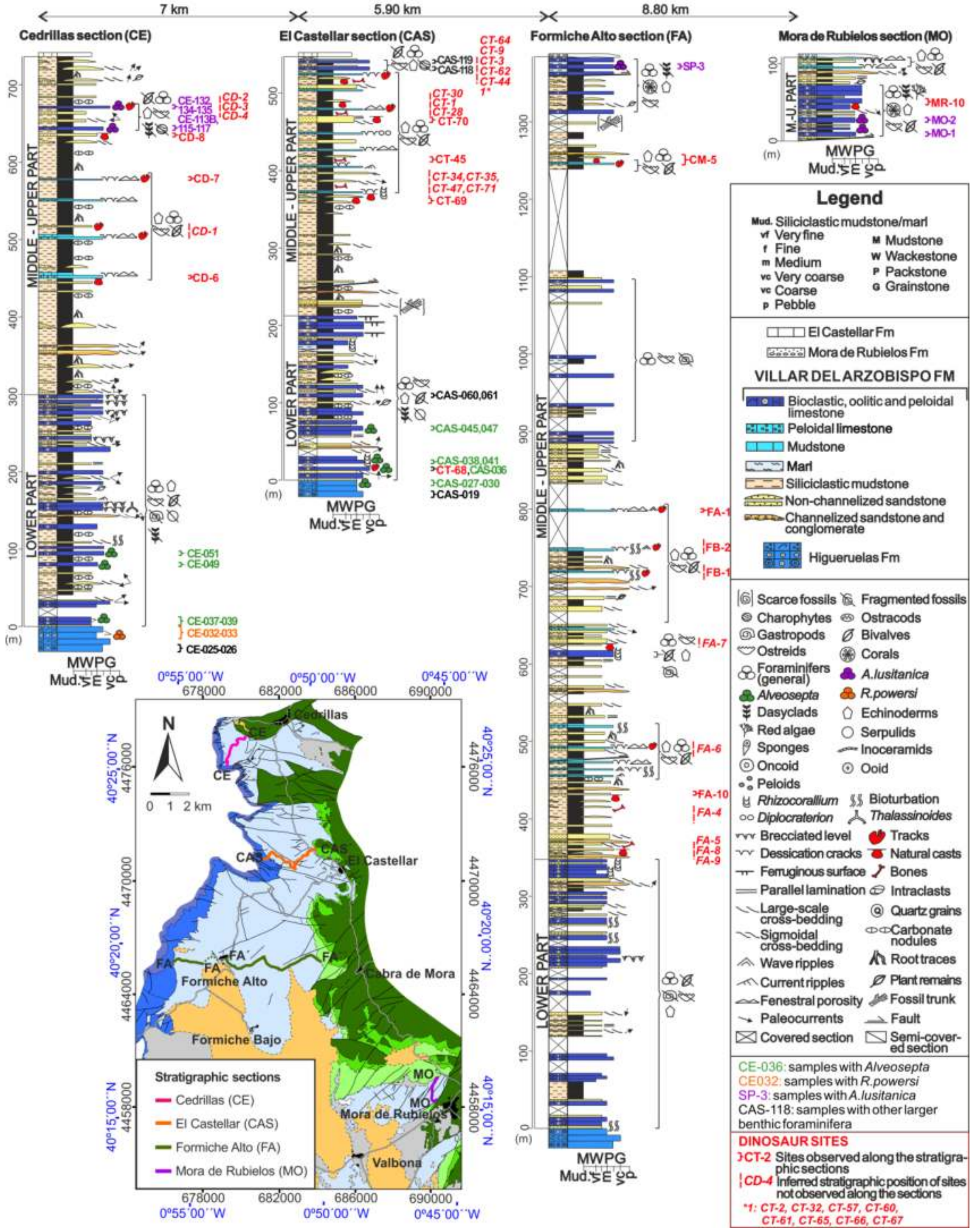
7 km
5.90 km
8.80 km
Cedrillas section (CE)
El Castellar section (CAS)
Formiche Alto section (FA)
Mora de Rubielos section (MO)
MIDDLE - UPPER PART
LOWER PART
M.-U. PART
Legend
Mud. Siliciclastic mudstone/marl
vf Very fine
f Fine
m Medium
vc Very coarse
vc Coarse
p Pebble
M Mudstone
W Wackestone
P Packstone
G Grainstone
El Castellar Fm
Mora de Rubielos Fm
VILLAR DEL ARZOBISPO FM
Bioclastic, oolitic and peloidal limestone
Peloidal limestone
Mudstone
Marl
Siliciclastic mudstone
Non-channelized sandstone
Channelized sandstone and conglomerate
Higueruelas Fm
Scarce fossils
Fragmented fossils
Charophytes
Ostracods
Gastropods
Bivalves
Ostreids
Corals
Foraminifers (general)
A.lusitanica
Alveosepta
R.powersi
Dasyclads
Echinoderms
Red algae
Serpulids
Sponges
Inoceramids
Oncoid
Ooid
Peloids
Rhizocorallium
Bioturbation
Diplocraterion
Thalassinoides
Brecciated level
Tracks
Dessication cracks
Natural casts
Ferruginous surface
Bones
Parallel lamination
Intraclasts
Large-scale cross-bedding
Quartz grains
Sigmoidal cross-bedding
Carbonate nodules
Wave ripples
Root traces
Current ripples
Plant remains
Fenestral porosity
Fossil trunk
Paleocurrents
Fault
Covered section
Semi-covered section
CE-036: samples with Alveosepta
CE032: samples with R.powersi
SP-3: samples with A.lusitanica
CAS-118: samples with other larger benthic foraminifera
DINOSAUR SITES
CT-2 Sites observed along the stratigraphic sections
CD-4 Inferred stratigraphic position of sites not observed along the sections
*1: CT-2, CT-32, CT-57, CT-60, CT-61, CT-65, CT-66, CT-67
Stratigraphic sections
Cedrillas (CE)
El Castellar (CAS)
Formiche Alto (FA)
Mora de Rubielos (MO)
Cedrillas
El Castellar
Formiche Alto
Cabra de Mora
Formiche Bajo
Mora de Rubielos
Valbona
0°55´00´´W
0°50´00´´W
0°45´00´´W
40°25´00´´N
40°20´00´´N
40°15´00´´N
0 1 2 km

Fig. 4

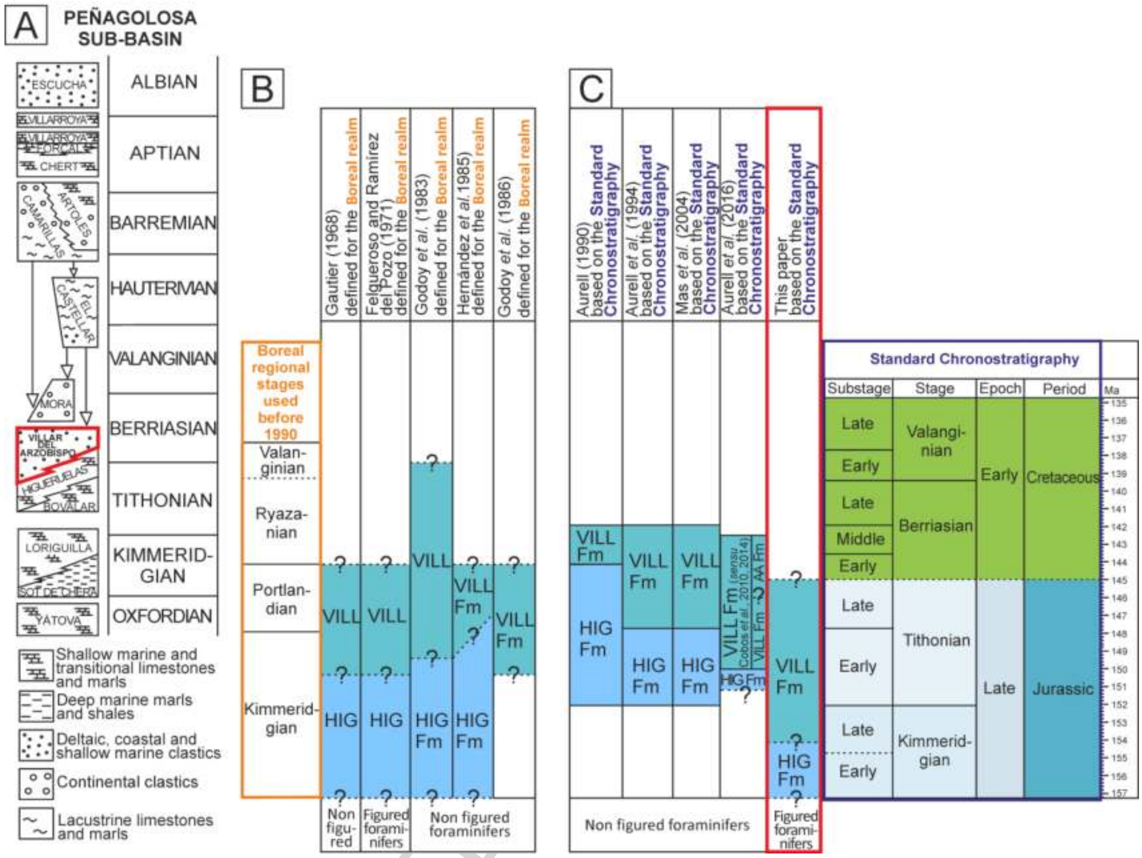
A
PEÑAGOLOSA SUB-BASIN
ALBIAN
APTIAN
BARREMIAN
HAUTERIVIAN
VALANGINIAN
BERRIASIAN
TITHONIAN
KIMMERID-GIAN
OXFORDIAN
ESCUCHA
VILLARROYA
FORCALL
CHERT
ARTOLES
CAMARILLAS
EL CASTELLAR
MORA
VILLAR DEL ARZOBISPO
HIGUERUELAS
BOVALAR
LORIGUILLA
SOT DE CHERA
YATOVA
Shallow marine and transitional limestones and marls
Deep marine marls and shales
Deltaic, coastal and shallow marine clastics
Continental clastics
Lacustrine limestones and marls
B
Boreal regional stages used before 1990
Valan-ginian
Ryaza-nian
Portlan-dian
Kimmerid-gian
Gautier (1968) defined for the Boreal realm
Felgueroso and Ramírez del Pozo (1971) defined for the Boreal realm
Godoy et al. (1983) defined for the Boreal realm
Hernández et al. 1985) defined for the Boreal realm
Godoy et al. (1986) defined for the Boreal realm
VILL
HIG
VILL Fm
HIG Fm
Non figu-red
Figured forami-nifers
Non figured foraminifers
C
Aurell (1990) based on the Standard Chronostratigraphy
Aurell et al. (1994) based on the Standard Chronostratigraphy
Mas et al. (2004) based on the Standard Chronostratigraphy
Aurell et al. (2016) based on the Standard Chronostratigraphy
This paper based on the Standard Chronostratigraphy
VILL Fm (sensu Cobos et al. 2010, 2014)
VILL Fm
AA Fm
HIG Fm
Non figured foraminifers
Figured forami-nifers
Standard Chronostratigraphy
Substage
Stage
Epoch
Period
Ma
Late
Early
Middle
Valangi-nian
Berriasian
Tithonian
Kimmerid-gian
Cretaceous
Jurassic

Fig. 5

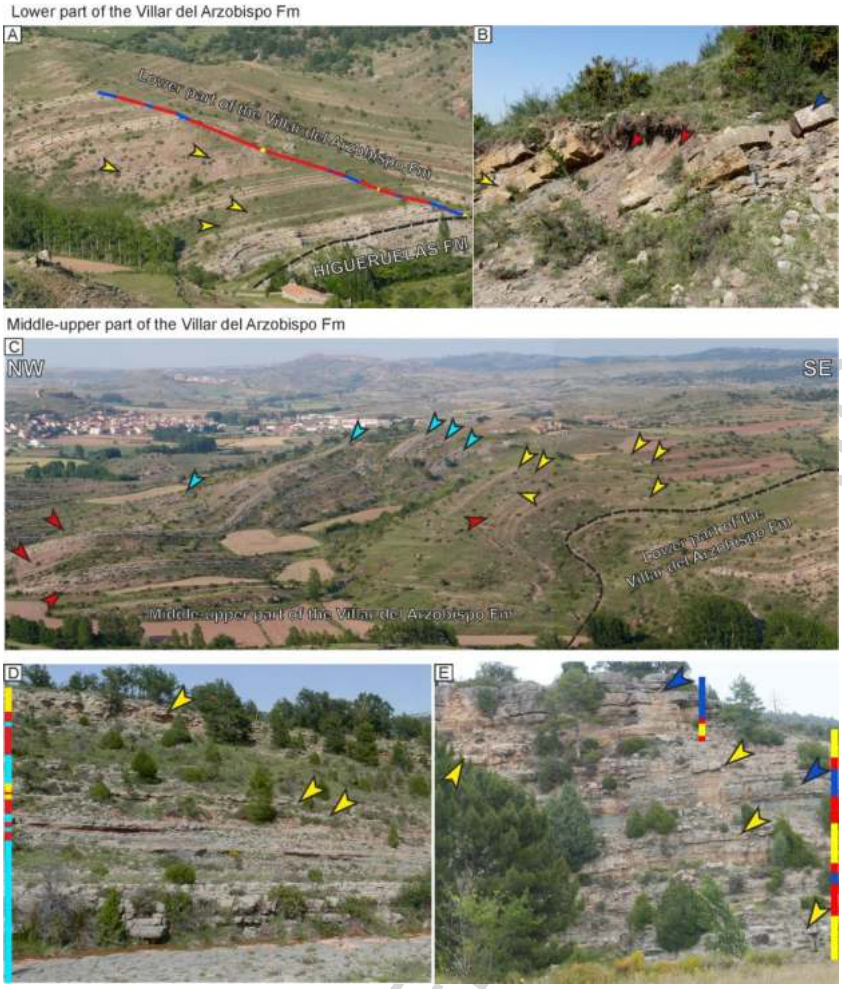
Lower part of the Villar del Arzobispo Fm
A
Lower part of the Villar del Arzobispo Fm
HIGUERUELAS FM
B
Middle-upper part of the Villar del Arzobispo Fm
C
NW
SE
Lower part of the Villar del Arzobispo Fm
Middle-upper part of the Villar del Arzobispo Fm
D
E

Fig. 6

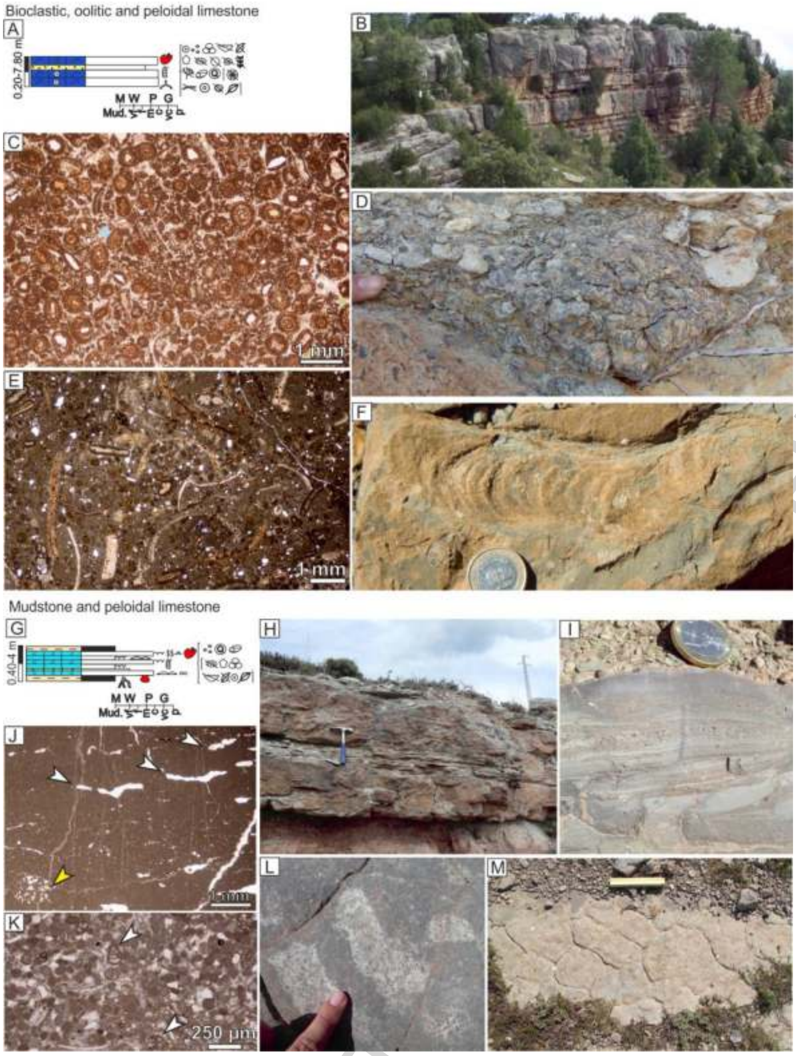
Bioclastic, oolitic and peloidal limestone
A
B
C
1 mm
D
E
1 mm
F
Mudstone and peloidal limestone
G
H
I
J
1 mm
K
250 μm
L
M

Fig. 7

Fig. 8

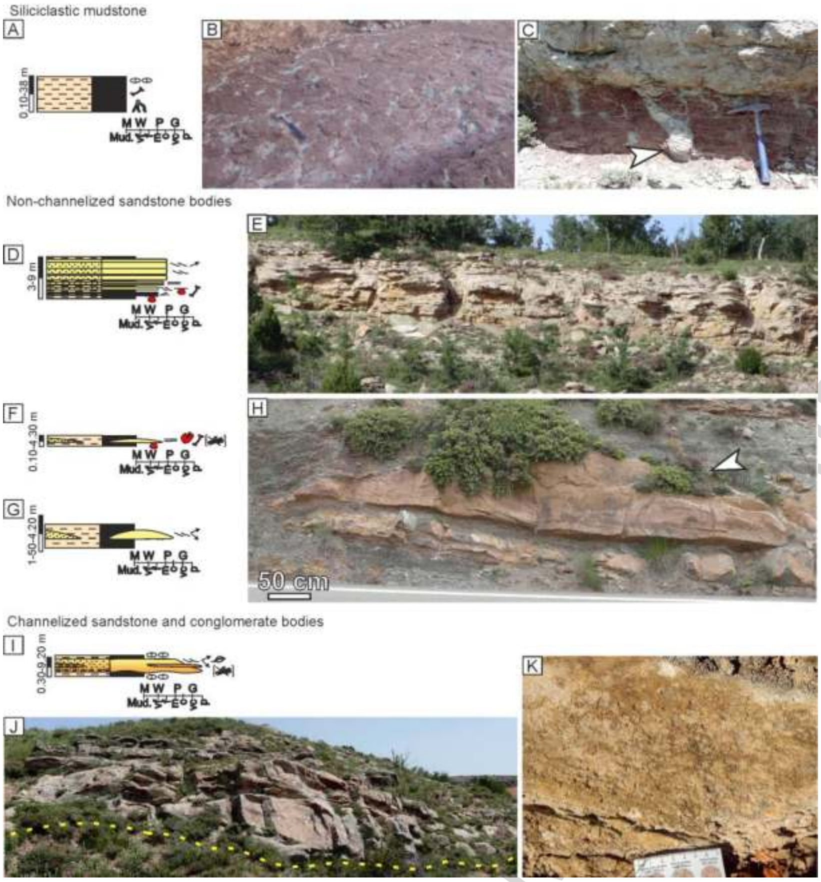
Siliciclastic mudstone
A
B
C
Non-channelized sandstone bodies
D
E
F
G
H
50 cm
Channelized sandstone and conglomerate bodies
I
J
K

Fig. 9

Fig. 10

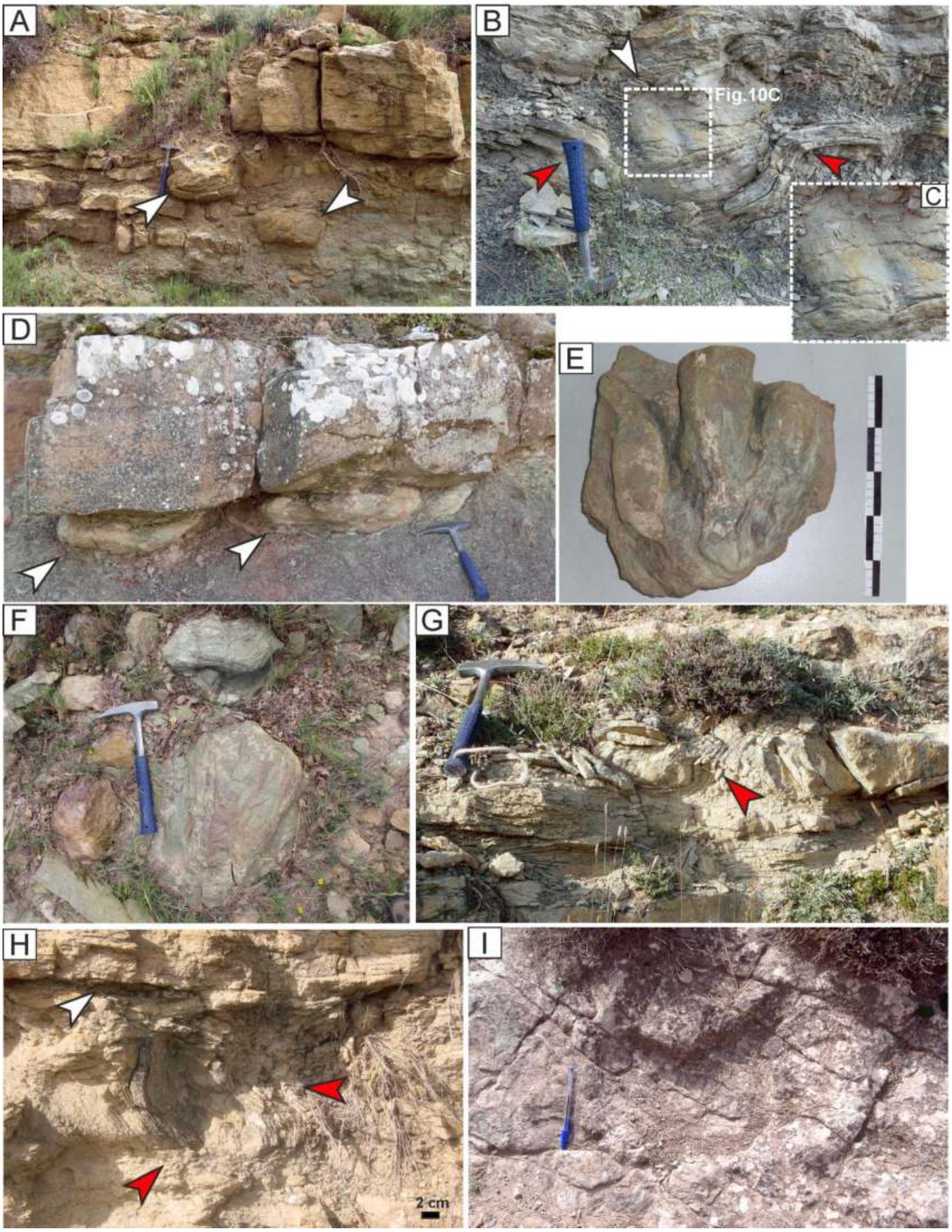

Fig. 11

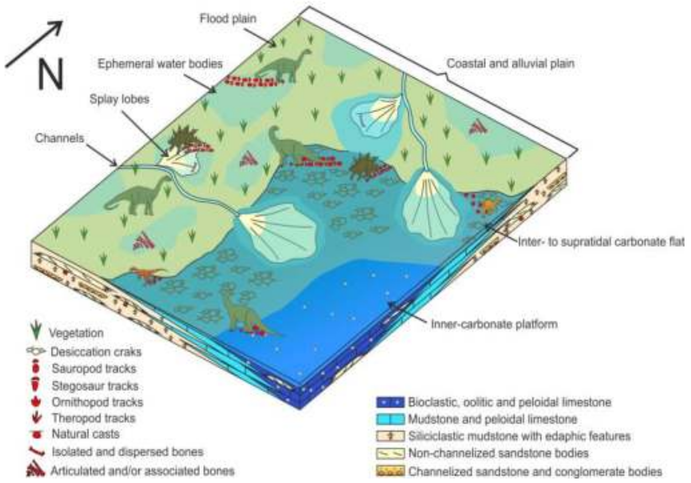
N
Flood plain
Ephemeral water bodies
Splay lobes
Channels
Coastal and alluvial plain
Inter- to supratidal carbonate flat
Inner-carbonate platform
Vegetation
Desiccation craks
Sauropod tracks
Stegosaur tracks
Ornithopod tracks
Theropod tracks
Natural casts
Isolated and dispersed bones
Articulated and/or associated bones
Bioclastic, oolitic and peloidal limestone
Mudstone and peloidal limestone
Siliciclastic mudstone with edaphic features
Non-channelized sandstone bodies
Channelized sandstone and conglomerate bodies

Fig. 12

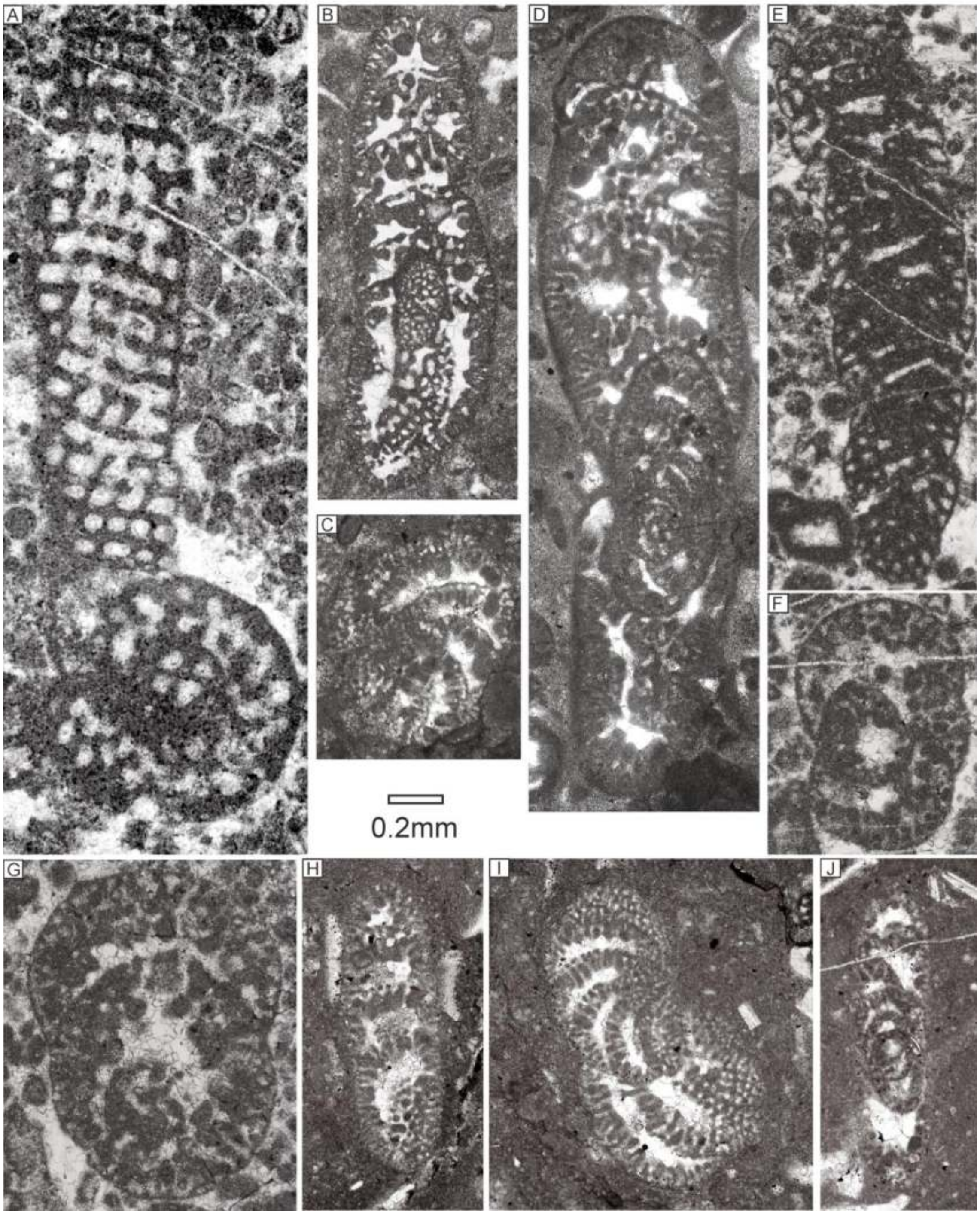

Fig. 13

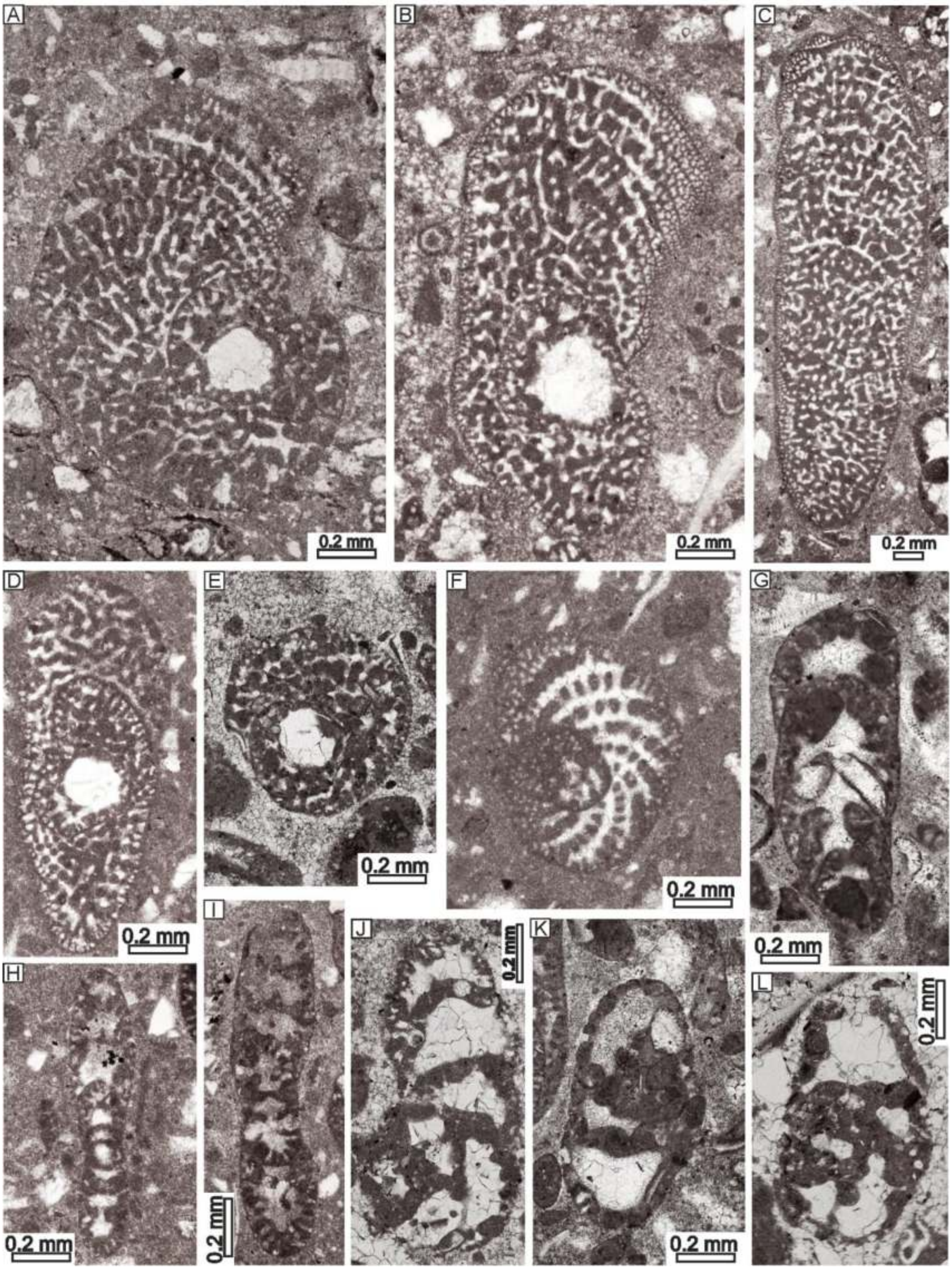
A
0.2 mm
B
0.2 mm
C
0.2 mm
D
0.2 mm
E
0.2 mm
F
0.2 mm
G
0.2 mm
H
0.2 mm
I
0.2 mm
J
0.2 mm
K
0.2 mm
L
0.2 mm

Table 1. Main dinosaur sites of the Villar del Arzobispo Formation in the Peñagolosa sub-basin.

Dinosaur site	Stratigraphic position	Facies	Type of fossils	Some references
CD-1 “La Masada”	Middle-upper part	Mudstone and peloidal limestone	Sauropod tracks	Cobos *et al*., 2008
CD-2 “Cedrillas”	Middle-upper part	Mudstone and peloidal limestone	Tracks	Cobos, 2011
CD-3 “Camino de Alcalá”	Middle-upper part	Mudstone and peloidal limestone	Stegosaurid? tracks	Cobos *et al*., 2012
CD-4 “La Curva”	Middle-upper part	Mudstone and peloidal limestone	Tracks	Cobos, 2011
CD-6	Middle-upper part	Mudstone and peloidal limestone	Tracks	This paper
CD-7	Middle-upper part	Mudstone and peloidal limestone	Tracks	Unpublished
CD-8	Middle-upper part	Non-channelized sandstone	Tracks	This paper
CT-1 “El Castellar”	Middle-upper part	Mudstone and peloidal limestone	Stegosaurid (*Deltapodus ibericus*) and theropod (e.g. *Iberosauripus grandis*) tracks	Alcalá *et al*., 2003; 2014b; Cobos *et al*., 2008; 2009; 2010; 2012; 2014
CT-2 “El Pozo”	Middle-upper part	Mudstone and peloidal limestone	Sauropod and ornithopod	Alcalá *et al*., 2003; 2014a;

			tracks	2014b Cobos *et al.*, 2008; 2012
CT-3 "Camino El Berzal"	Middle-upper part	Mudstone and peloidal limestone	Sauropod and theropod tracks	Alcalá *et al.*, 2003; 2014; Cobos *et al.*, 2014
CT-9 "Berzal Norte"	Middle-upper part	Non-channelized sandstone	Bones	Unpublished
CT-28 "San Cristóbal"	Middle-upper part	Siliciclastic mudstone	Stegosaurid bones (*Dacentrurus*)	Cobos *et al.*, 2009; 2010
CT-30 "La Tejería"	Middle-upper part	Siliciclastic mudstone	Sauropod bones	This paper
CT-32 "La Balsa"	Middle-upper part	Mudstone and peloidal limestone	Stegosaurid? tracks	Cobos *et al.*, 2008; 2012
CT-34	Middle-upper part	Non-channelized sandstone	Bones	Unpublished
CT-35	Middle-upper part	*Ex situ*	Bones	Unpublished
CT-44 "El Pajar"	Middle-upper part	Mudstone and peloidal limestone	Tracks	Cobos, 2011
CT-45 "Costillas"	Middle-upper part	Siliciclastic mudstone	Bones	This paper
CT-47	Middle-upper part	Siliciclastic mudstone	Bones	This paper
CT-57	Middle-upper	Non-channelized	Theropod tracks	This paper

	part	sandstone		
CT-60 "Los Canales"	Middle-upper part	Siliciclastic mudstone	Diplodocoidea bones	Cobos *et al*., 2015
CT-61	Middle-upper part	Non-channelized sandstone	Bones and tracks	This paper
CT-62 "La Carrasca"	Middle-upper part	Non-channelized sandstone	Tracks	This paper
CT-64	Middle-upper part	Mudstone and peloidal limestone	Stegosaurid tracks "*Deltapodus*-like"	This paper
CT-65	Middle-upper part	Non-channelized sandstone	Tracks	Unpublished
CT-66	Middle-upper part	Non-channelized sandstone	Tracks	Unpublished
CT-67	Middle-upper part	Non-channelized sandstone	Tracks	Unpublished
CT-68 "Corral de Igualdo"	Lower part	Bioclastic and oolitic limestone	Tracks	This paper
CT-69	Middle-upper part	Non-channelized sandstone	Tracks	Unpublished
CT-70	Middle-upper part	Non-channelized sandstone	Tracks	Unpublished
CT-71	Middle-upper	Mudstone and	Tracks	Unpublished

"Barraca Baja"	part	peloidal limestone		
FB-1 "El Molino"	Middle-upper part	Mudstone and peloidal limestone	Sauropod tracks	Cobos *et al*., 2005
FB-2 "Camino de Cabra"	Middle-upper part	Mudstone and peloidal limestone	Sauropod and theropod tracks	Cobos *et al*., 2005
FA-1 "Barranco de los Arcos"	Middle-upper part	Mudstone and peloidal limestone	Sauropod and theropod tracks	Cobos *et al*., 2005
FA-4	Middle-upper part	Non-channelized sandstone e	Bones	Unpublished
FA-5 "Masía de la Hoya Alta"	Middle-upper part	*Ex situ*	Megalosauridae tooth	Cobos *et al*., 2014; 2015
FA-6 "Masía de la Cañada"	Middle-upper part	Mudstone and peloidal limestone	Ornithopod and sauropod tracks	Cobos *et al*., 2015
FA-7	Middle-upper part	Non-channelized sandstone	Tracks	This paper
FA-8	Middle-upper part	Non-channelized sandstone	Tracks	This paper
FA-9	Middle-upper part	Non-channelized sandstone	Tracks	Unpublished
FA-10	Middle-upper	Non-channelized	Tracks	Unpublished

	part	sandstone		
CM-5	Middle-upper part	Mudstone and peloidal limestone, non-channelized sandstone	Tracks	Unpublished
MR-10	Middle-upper part	Bioclastic and oolitic limestone	Tracks	This paper

* See Fig. 2 for exact location of each dinosaur site